AD-A045 534 MCDONNELL DOUGLAS RESEARCH LABS ST LOUIS MO F/G 11/9
THE DURABILITY OF EPOXIES.(U)
AUG 77 R J MORGAN, J E O'NEAL F44620-76-C-0075
UNCLASSIFIED MDC-00631 NL

| OF |
AD
A045534

END
DATE
FILMED
11-77
DDC

MCDONNELL DOUGLAS RESEARCH LABORATORIES

MCDONNELL DOUGLAS CORPORATION

UNCLASSIFIED
SECURITY CLASSIFICATION OF THIS PAGE (When Data Entered)

REPORT DOCUMENTATION PAGE

READ INSTRUCTIONS BEFORE COMPLETING FORM

1. REPORT NUMBER

2. GOVT ACCESSION NO. (9)

3. RECIPIENT'S CATALOG NUMBER

4. TITLE (and Subtitle) (6)
THE DURABILITY OF EPOXIES

5. TYPE OF REPORT & PERIOD COVERED
Interim Report
1 Apr 1976-30 Apr 1977

6. PERFORMING ORG. REPORT NUMBER (14)
MDC-Q0631

7. AUTHOR(s) (10)
R. J. Morgan
J. E. O'Neal

8. CONTRACT OR GRANT NUMBER(s) (15)
F44620-76-C-0075

9. PERFORMING ORGANIZATION NAME AND ADDRESS
McDonnell Douglas Research Laboratories
McDonnell Douglas Corporation
St. Louis, MO 63166

10. PROGRAM ELEMENT, PROJECT, TASK AREA & WORK UNIT NUMBERS (16) (17)
2303/A3 61102F

11. CONTROLLING OFFICE NAME AND ADDRESS
Air Force Office of Scientific Research/NC
Bolling Air Force Base, DC 20332

12. REPORT DATE (11)
1 August 1977

13. NUMBER OF PAGES
79

14. MONITORING AGENCY NAME & ADDRESS (if different from Controlling Office)
(12) 78p.

15. SECURITY CLASS. (of this report)
Unclassified

15a. DECLASSIFICATION/DOWNGRADING SCHEDULE

16. DISTRIBUTION STATEMENT (of this Report)

Approved for public release; distribution unlimited

17. DISTRIBUTION STATEMENT (of the abstract entered in Block 20, if different from Report)

18. SUPPLEMENTARY NOTES

19. KEY WORDS (Continue on reverse side if necessary and identify by block number)

Epoxies	Failure modes	Swelling
Durability	Crazing	Fabrication stresses
Network structure	Sorbed moisture	Environmental stresses
Microvoids	Glass transition	
Deformation modes	Diffusion	

20. ABSTRACT (Continue on reverse side if necessary and identify by block number)

This report reviews the state of knowledge of the basic factors that control the durability of epoxies in service environments. The structure-property relations of amine (diethylene triamine, DETA)-cured bisphenol-A-diglycidyl ether (DGEBA) and amine (diaminodiphenyl sulfone, DDS)-cured tetraglycidyl 4,4'diaminodiphenyl methane (TGDDM) epoxies, the effects of sorbed moisture, and the fabrication and environmental factors that control the durability of epoxies are reviewed. The modes of deformation and failure of these materials, which occur primarily by crazing, are controlled by their network

DD FORM 1 JAN 73 1473 EDITION OF 1 NOV 65 IS OBSOLETE

UNCLASSIFIED
SECURITY CLASSIFICATION OF THIS PAGE (When Data Entered)

405 315

20. Abstract (Continued)

structure and microvoid characteristics. The pertinent, basic, physical phenonema induced and/or modified by sorbed moisture that affect the durability of epoxies are reviewed. These include the plasticization, swelling stresses, and modification of the crazing process in epoxies caused by sorbed moisture together with the diffusion characteristics of moisture in these materials. The durability of epoxies in service environments are discussed in terms of the structure-property relations of epoxies, the effect of fabrication and environmental factors, and their complex interactions on the formation of permanent damage regions.

PREFACE

This McDonnell Douglas Research Laboratory (MDRL) report reviews the phenomena which control the durability of epoxies. The MDRL epoxy studies initially were performed under the McDonnell Douglas Independent Research and Development program and during 1976 under Air Force contract F44620-76-C-0075, entitled "The Relation Between the Chemical and Physical Structure and the Mechanical Response of Polymers" (1 April 76-28 February 77) which is monitored by Dr. D. R. Ulrich, Chemical Sciences Directorate, Air Force Office of Scientific Research. The details of these studies are presented in the references quoted.

This report has been reviewed and is approved.

D. P. Ames for C. J. Wolf

C. J. Wolf
Chief Scientist, Chemical Physics
McDonnell Douglas Research Laboratories

D. P. Ames

D. P. Ames
Staff Vice President
McDonnell Douglas Research Laboratories

TABLE OF CONTENTS

LIST OF ILLUSTRATIONS

LIST OF TABLES

1. INTRODUCTION

Epoxies are utilized by the aerospace industry primarily in the form of matrices for composite materials and as adhesives. The increasing use of epoxies requires a knowledge of their lifetime in extreme service environments. When epoxy adhesives and composites are utilized in primary structural components of airframes, it is vital that the durability of such components be known during design development. A number of laboratory and field studies have indicated that the combined effects of sorbed moisture and thermal environment can cause significant changes in the mechanical response of these materials.[1,2] However, the long-term, in-service durability of epoxy adhesives and composites in primary structural airframe components is unknown primarily because (1) long-term, in-service aging characteristics are difficult to simulate by short-term laboratory and/or field tests and (2) the basic phenomena responsible for the changes in the mechanical response in laboratory-simulated service environments have not been identified and/or understood.

To predict the durability of epoxies in a service environment with confidence requires knowledge of (1) the chemical structure and the physical arrangement of the crosslinked network structure in the bulk, (2) the molecular nature of the flow and failure processes, (3) the structural parameters which control the flow and failure processes, (4) the effect of the flow and failure processes on the mechanical properties, and (5) how these structural parameters are modified by fabrication procedures and the service environment. These basic relationships are illustrated in Figure 1. To predict the durability of an epoxy in a specific environment requires identification of the primary failure mode, if any, and the structural phenomena controlling the initiation and growth characteristics of this mode. Identification of the primary failure mode, which may be difficult, and subsequent durability predictions require a thorough understanding of the relationships illustrated in Figure 1.

In this report, we review the basic areas necessary for meaningful durability predictions: (1) the structure of epoxies, (2) their modes of deformation and failure and the structural parameters controlling these modes, (3) the effects of sorbed moisture on the epoxy structure, properties, and modes of deformation and failure, and (4) the complex fabrication and environmental phenomena affecting the durability in service environments.

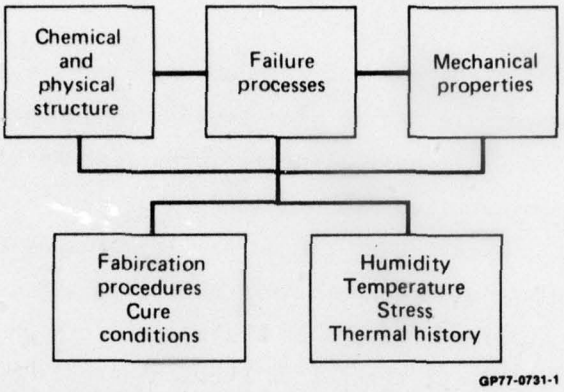

Figure 1 The basic epoxy interrelationships necessary for durability predictions

2. CONCLUSIONS

The structure-property relations of TGDDM-DDS and DGEBA-DETA epoxies, the effects of sorbed moisture, and the fabrication and environmental factors that control the durability of epoxies have been reviewed. The primary conclusions are summarized as follows.

2.1 Structure-Property Relations

- The modes of deformation and failure and mechanical response of epoxies are controlled by the epoxy network structure and microvoid characteristics.

- The crosslink-density distribution in epoxy networks can be heterogeneous with regions of low-crosslink density controlling the flow processes. Steric and diffusional restrictions inhibit crosslink reactions during the latter stages of cure and limit the overall achievable crosslink density.

- Microvoids, which act as stress concentrations and sinks for sorbed moisture, can be formed in epoxies as a result of clusters of unreacted, low-molecular-weight material ejected from the epoxies during cure.

- The epoxies deform and fail predominantly by a crazing process. The TGDDM-DDS epoxies also deform to a limited extent by shear banding.

2.2 Sorbed Moisture

- Epoxies are plasticized by sorbed moisture, and their T_g's are lowered to a greater extent than predicted from free-volume considerations. Strong hydrogen bonding or the preferential accumulation of moisture in regions of low-crosslink density could explain the anomalous plasticization.

- Moisture diffusion in epoxies can be adequately described by Fick's laws of diffusion. Non-Fickian diffusion with accelerated moisture sorption will occur, however, in environments that cause microvoid or crack formation in the epoxies.

- Local swelling stresses generated by the sorption of moisture in epoxies cannot be predicted accurately without a detailed knowledge of the epoxy network structure and the moisture distribution within the network.

- Sorbed moisture enhances the craze cavitation and propagation processes in the epoxies by plasticization. The craze cavitation stress is

more susceptible to sorbed moisture than T_g, particularly when microscopic regions of high-moisture concentration are present in the epoxy. Therefore, modification of T_g by sorbed moisture cannot alone be utilized as a sensitive guide to predict deterioration in the mechanical response and durability of epoxies.

2.3 Durability

● Permanent damage regions can form on the surface of epoxy components when aircraft perform supersonic maneuvers. Such maneuvers can impose surface tensile stresses greater than the epoxy craze cavitation stress as a result of severe temperature and moisture gradients.

● To predict the durability of epoxies with confidence in less extreme environmental conditions requires a detailed knowledge of the service environment, the structure-property relations of epoxies, the effect of fabrication and environmental factors, and their complex interactions on the formation of permanent damage regions. The present knowledge of epoxies and composite materials is not sufficiently advanced to achieve accurate predictions.

3. RECOMMENDATIONS

For accurate durability predictions of epoxies, additional studies are required to determine:

(1) the effect of cure conditions on the network structure and microvoid characteristics,

(2) the relation between network structure and modes of deformation and failure,

(3) the relation between the crazing process and fatigue characteristics,

(4) the local swelling stresses for different network morphologies and moisture distributions,

(5) the molecular interactions of water molecules with polymer chains,

(6) the effect of inhomogeneous diluent concentrations on the solvent crazing process,

(7) the magnitude of fabrication stresses for specific cure conditions,

(8) the total stresses imposed on an epoxy as a result of combined service, fabrication, and environmental stresses as a function of specific environments, and

(9) the identification of the critical path to failure for specific environments.

4. STRUCTURE OF EPOXIES

The mechanical response of a polymer glass depends on the amount of flow occurring during the failure process, either microscopically via crazing and/or shear banding or macroscopically via necking.[2-15] Hence, it is important to identify the major structural parameters controlling the flow processes that occur during deformation and failure. The major parameters controlling the flow processes in uncrosslinked polymer glasses are the free volume[16-21] and the stress-raising microvoid characteristics of the glass[19,22,23]. For crosslinked glasses, such as epoxies, the crosslinked network structure is an additional structural parameter affecting the flow processes.

4.1 Network Structure

Generally, the cure process and final network structure of epoxies have been estimated from (1) the chemistry of the system, if the curing reactions are known and assumed to go to completion, and (2) experimental techniques such as infrared spectra, swelling, dynamic mechanical, thermal conductivity, and differential scanning calorimetry measurements.[24-39] However, in many epoxy systems, the chemical reactions are diffusion controlled and incomplete, and a heterogeneous distribution in the crosslink density occurs. Both of these factors significantly modify the network structure. Figure 2 schematically illustrates possible network topographies of epoxies.[40,41,62] An ideal uniform-crosslinked network structure is illustrated in Figure 2(a). In reality, however, networks contain loops and dangling chain-ends as illustrated in Figure 2(b). Such networks can exhibit essentially a uniform-crosslink density in a low-molecular-weight or crosslink density matrix [Figure 2(c)]. Also, non-uniform crosslink density networks in which regions of high-crosslink density form either a continuous [Figure 2(d)] or a discontinuous phase in a low-molecular-weight or crosslink density matrix are other possible network morphologies.

High-crosslink density regions from 6 to 10^4 nm in diameter have been observed in crosslinked resins.[19,26,42-60] The conditions for formation of a heterogeneous rather than a homogeneous system depend on polymerization conditions (i.e., temperature, solvent, and/or chemical composition). The high-crosslink density regions have been described as agglomerates of colloidal particles[47,48] or floccules[50] in a lower-molecular-weight interstitial fluid.

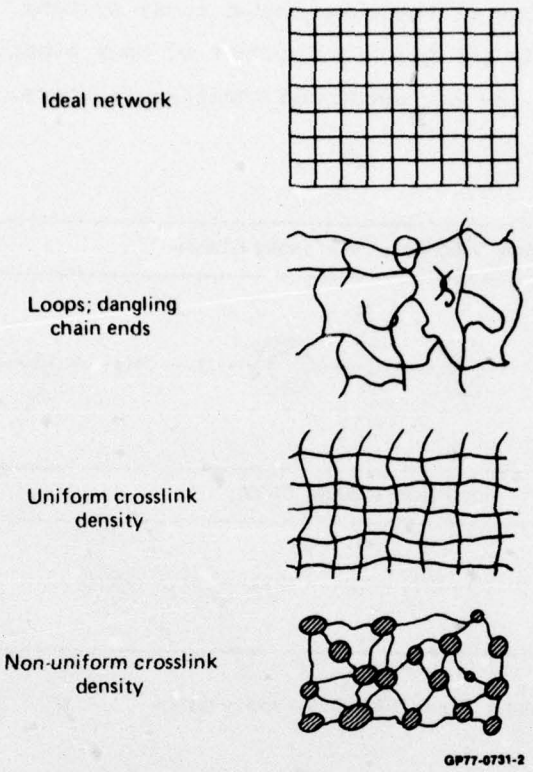

Figure 2 Epoxy network morphologies (Reference 62)

Solomon et al.[49] suggested that a two-phase system is produced by microgelation prior to the formation of a macrogel. Kenyon and Nielson[28] suggested that the highly-crosslinked microgel regions are loosely connected during the latter stages of the curing process. More recently, Karyakina et al.[58] suggested that microgel regions originate in the initial stages of polymerization from the formation of micro-regions of aggregates of primary polymer chains. The high-crosslink density regions have been reported to be only weakly attached to the surrounding matrix[47,48,50], and their size varies with cure conditions[47], proximity of surfaces[50,57], and the presence of solvents[28,49].

The epoxy network structure depends on the chemistry of the system, the initial epoxy:curing agent ratio, and cure conditions. In this report, we consider two chemically different epoxy systems: (1) an amine (diethylene triamine, DETA)-cured difunctional bisphenol-A-diglycidyl ether epoxy (DGEBA) (Figure 3) and (2) an amine (diaminodiphenyl sulfone, DDS)-cured tetrafunctional tetraglycidyl 4,4'-diaminodiphenyl methane epoxy (TGDDM) (Figure 4). The

DGEBA-DETA epoxy system is one of the more common epoxy systems, whereas the TGDDM-DDS system is currently the main constituent of many adhesives and composite matrices utilized by the Air Force and their contractors.

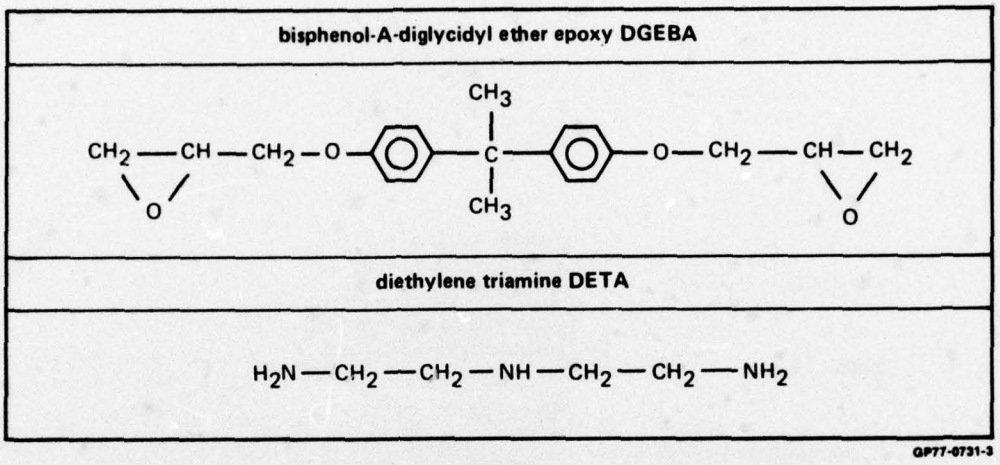

Figure 3 The DGEBA-DETA epoxy system

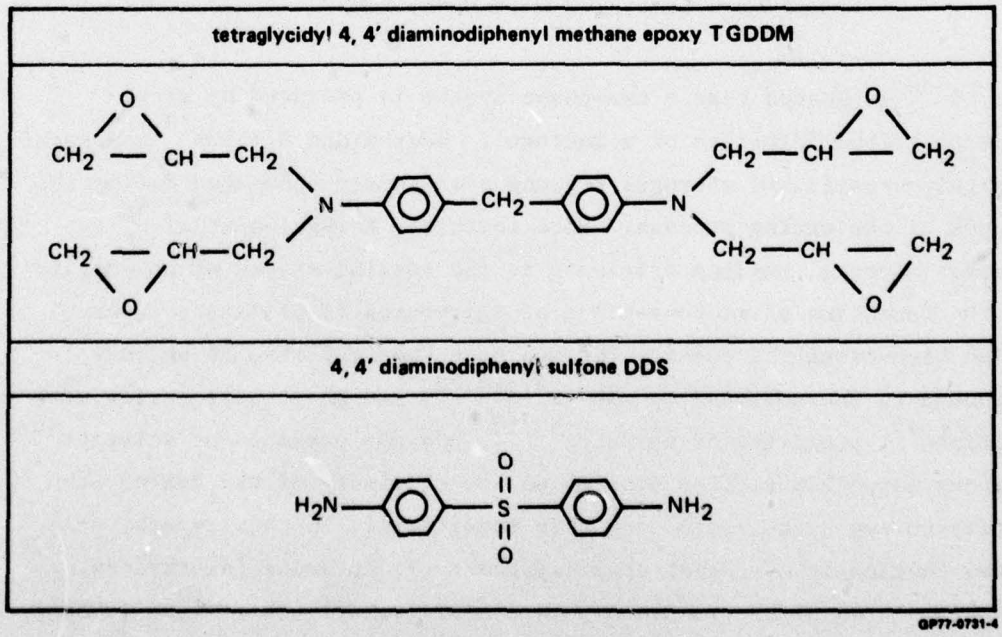

Figure 4 The TGDDM-DDS epoxy system

4.1.1 The DGEBA-DETA Epoxy System

The stoichiometric mixture for the DGEBA-DETA epoxy system is ∿ 11 wt% DETA.[61] This composition was determined by assuming that all primary and secondary amine hydrogens react with epoxide groups in absence of side reactions. However, DGEBA-DETA epoxies, despite being prepared from stoichiometric mixtures of epoxy and amine, are not highly crosslinked glasses because they exhibit 15-20% extension to break 25°C below their T_g's. Also, considerable molecular flow occurs during the deformation and failure of these glasses.

Furthermore, the mechanical properties of these epoxies exhibit a free-volume dependence as a function of thermal history which indicates that these glasses consist of regions of lightly or non-crosslinked material. A typical volume-temperature plot for a polymer is shown in Figure 5. Changes in free volume, or local order, in the glassy state can occur as a result of extension to temperatures below T_g of packing changes associated with the liquid state. The liquid-volume temperature plot extrapolated to below T_g in Figure 5 represents the lower free-volume, equilibrium state of the glass. The time necessary to achieve the equilibrium state at a given temperature below T_g depends on the glassy-state mobility. Below a certain temperature, the glassy-state mobility is too small to allow any changes in free volume. A decrease in free volume that occurs in the glassy state results in inhibition of the flow processes that take place during deformation and a more brittle mechanical response. Rapidly cooling from above T_g, however, produces a glass with a larger free volume.

Table 1 shows the effect of thermal history on the room-temperature tensile yield stress and ultimate elongation of a DGEBA-DETA (13 wt% DETA) epoxy glass (T_g ∿ 107°C). Annealing 5°C below T_g (specimens 1-5 in Table 1) causes an increase in the macroscopic yield stress and a decrease in the extension to break as the equilibrium state of the glass at this temperature is approached. Prior to testing, samples 6,7, and 8 in Table 1 were exposed to the same thermal history as preceding samples in this 6 to 8 series. Quenching from 55°C above T_g (specimen 6 in Table 1) produces a low macroscopic yield stress because of the high free-volume frozen into the glass. Subsequent annealing of the quenched specimen in the glassy state 5°C below T_g (102°C) (specimen 7 in Table 1)followed by a further quench from 55°C above T_g (specimen

8 in Table 1) produces essentially reversible changes in the macroscopic yield stress. These modifications of the macroscopic yield stress and ultimate elongation with thermal history indicate that the flow processes in DGEBA-DETA epoxies are controlled by the free volume of the regions of lightly or non-crosslinked material.

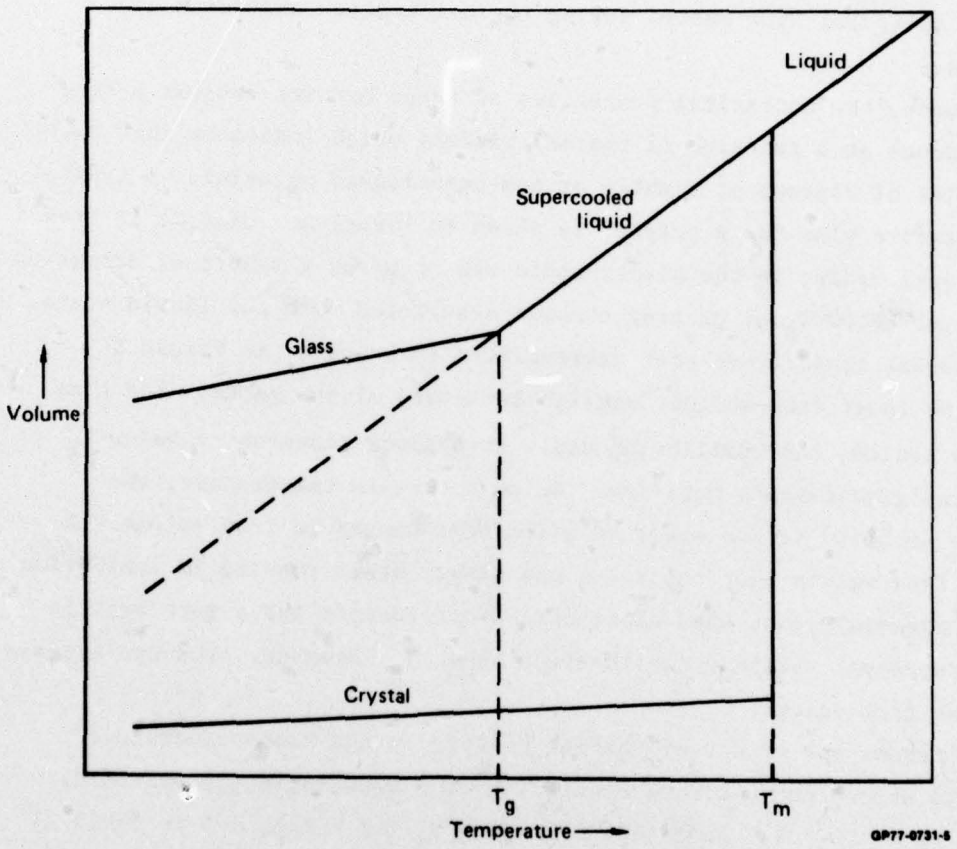

Figure 5 A schematic volume-temperature plot for a polymer

TABLE 1 EFFECT OF THERMAL HISTORY ON THE ROOM-TEMPERATURE TENSILE MECHANICAL PROPERTIES (STRAIN RATE ~ 10^{-2}/min) OF DETA (13 wt%)-CURED DGEBA EPOXY.

Thermal history	Yield stress (kPa x 10^4)	Ultimate elongation (%)
1) Cured 24 h, 23°C; 24 h, 150°C; cooled 2°C/min to room temperature	7.9 ± 0.1	14 ± 1
2) 102°C - 1 day	8.2 ± 0.1	14 ± 1
3) 102°C - 3 days	8.2 ± 0.1	13 ± 1
4) 102°C - 6 days	8.2 ± 0.1	12 ± 1
5) 102°C - 17 days	8.2 ± 0.1	11 ± 1
6) 162°C, 10 min; quenched in ice water	7.3 ± 0.1	15 ± 1
7) 102°C - 1 day	8.3 ± 0.1	13 ± 1
8) 162°C, 10 min; quenched in ice water	7.3 ± 0.1	17 ± 1

GP77-0731-35

Figure 6 illustrates the effect of annealing [5°C below T_g (125°C)] on the temperature and strain-rate dependence of the macroscopic yield stress of DGEBA-DETA (11 wt% DETA) epoxy relative to the unannealed epoxy. The general increase in the yield stress at all temperatures and strain-rates on annealing below T_g further illustrates the free-volume dependence of these epoxies.

The DGEBA-DETA epoxies did not significantly swell (maximum swell ratio achieved $\simeq$ 1.5%) after 15 days exposure to the favorable swelling agents reported for similar materials.[25] The literature also suggests that swelling is not a valid technique to determine crosslink density of resins prepared from approximately stoichiometric quantities of epoxy and amine.[26,28,62] The lack of swelling does suggest, however, that these glasses are highly crosslinked.

The lack of swelling the high-temperature ductility, and the free-volume dependence of the mechanical properties of DGEBA-DETA epoxies can be understood if these glasses possess a heterogeneous-crosslink density distribution. We suggest that these glasses consist of regions of high-crosslink density interconnected by free-volume dependent, low-crosslinked or non-crosslinked material. The latter control the flow properties of these epoxies.

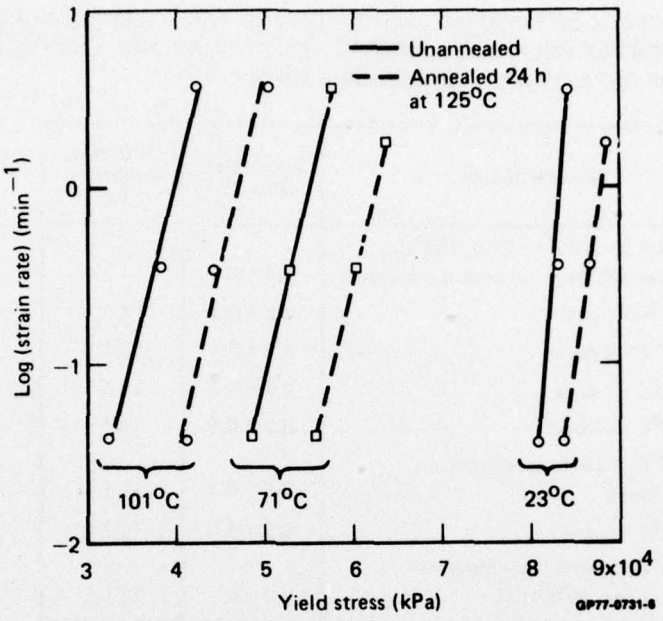

Figure 6 Log (strain-rate) versus yield stress of a DGEBA-DETA (11 wt% DETA) epoxy as a function of temperature and thermal history

This morphological model is consistent with bright-field transmission electron microscope observations. The bright-field transmission electron micrographs in Figure 7 show the network structure of interconnected 6-9 nm diameter particles observed in a strained DGEBA-DETA epoxy film. By straining the epoxy films directly in the electron microscope, we observed that the 6-9 nm diameter particles remain intact and flow past one another during the flow processes. The basic 6-9 nm diameter particles shown in Figure 7 are in the size range associated with molecular domains. For crystallizable polymers, Wunderlich and Mehta[63] and Aharoni[64] have presented theories in which the initial step of crystallization from the melt and solution occurs by formation of ordered molecular domains. Ordered nodules the size of molecular domains (5-6 nm in diameter) have been observed in thin films and on the surfaces of polycarbonate.[21,65] We suggest that the 6-9 nm diameter particles are molecular domains which are intramolecularly crosslinked and which form during the initial stages of polymerization. Chompff[66] has recently noted that configurational restrictions favor excessive intramolecular crosslinking. Intramolecular crosslinking is also favored by the inability of many unreacted

epoxy and amine species attached to a growing domain to diffuse to reactive species attached to neighboring domains. These species therefore can react only with active species in their immediate location. The intramolecularly-crosslinked molecular domains are interconnected by either low- or high-crosslink density regions during the latter stages of the cure to form the final network structure. This hypothesis assumes that intramolecular crosslinking occurs in the early polymerization stages. For solution-phase condensation crosslinking, Flory[67] considered intramolecular crosslinking insignificant prior to gelation. Other workers, however, caution that in many thermoset systems, intramolecular crosslinking could occur to a significant extent prior to gelation[68-70]. The ability of the suggested 6-9 nm diameter molecular domains to remain intact during the flow processes does, however, suggest that intramolecular crosslinking occurred within the domains.

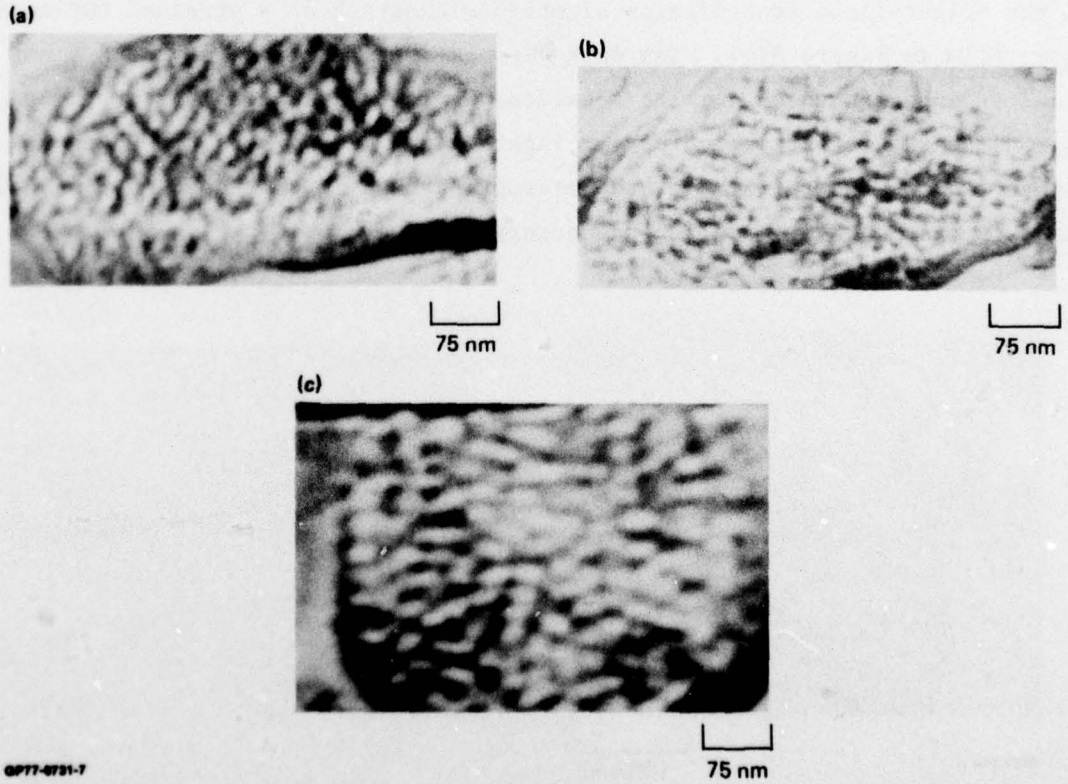

Figure 7 Bright-field transmission electron micrographs of network structure in deformed DGEBA-DETA (13 wt% DETA) epoxies

The interconnection of molecular domains by regions of either low- or high-crosslink density allows two types of network structure: (1) regions of high-crosslink density embedded in a low- or non-crosslinked matrix or (2) non-crosslinked or low-crosslink density regions embedded in a high-crosslink density matrix. From straining films in the electron microscope, we have observed both types of network morphology, with the second type more prevalent. An example of the first type of morphology is illustrated in Figure 8(a) where aggregates of 6-9 nm particles are embedded in a deformable, low-crosslink density matrix. Deformation of this type of network involves preferential deformation of the regions of low-crosslink density without causing cleavage of the high-crosslink regions. For the second type of network, the deformation process is more complex. Local affine deformation requires network cleavage and flow to occur simultaneously in the high-crosslink density regions as flow with little network cleavage occurs in the neighboring low-crosslink density regions. This deformation process results in progressively larger regions that are poorly crosslinked. Such a deformed network structure is illustrated in the bright-field transmission electron micrograph of a strained DGEBA-DETA epoxy film in Figure 8(b). The dark network structure consists of 6-9 nm diameter interconnected domains separated by low-crosslinked and/or thinned regions of the network which appear light in the micrograph. The network is tighter in the bottom-right of the micrograph than in the upper portion which suggests that more deformation has occurred there.

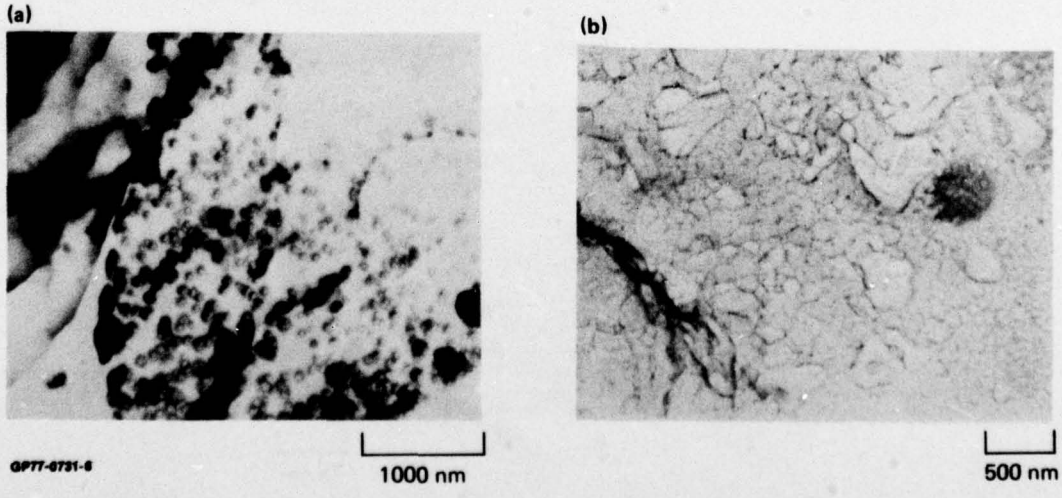

Figure 8 Bright-field transmission electron micrographs of strained DGEBA-DETA epoxies illustrating (a) aggregates of 6-9 nm particles in a low-crosslink density matrix and (b) a network in which high-crosslink density regions form the continuous phase

The presence of regions of low-crosslink density in the DGEBA-DETA epoxies suggests that many reactive groups remain unreacted within these glasses because of diffusion and steric restrictions imposed during polymerization and network formation.

Studies have not yet been performed on the effect of different cure conditions on the network structure. The room-temperature mechanical properties of DETA-DGEBA epoxies, however, do not vary as a function of post-cure temperature when post-cured for 24 h in vacuum at 80°-190°C.[71] Despite the presence of regions of low-crosslink density containing unreacted groups, diffusion and steric restrictions inhibit additional crosslinking in this temperature range. However, exposure to temperatures above 180°C for 24 h, where diffusional and steric restrictions may be partially overcome, causes the epoxies to embrittle because of the onset of complex oxidative crosslinking reactions. Differential infrared analysis of an epoxy post-cured above 180°C relative to a standard epoxy post-cured at 150°C reveals an additional broad sorption band in the 700-1800 cm^{-1} region.[71] The intensity of this sorption increased with exposure time and increasing temperature, from 180°-300°C, and increased more rapidly in air than in vacuum. A strong infrared sorption at 1725 cm^{-1} appears during the initial stages of the degradation process, which indicates the formation of carbonyl groups. Such groups could result from oxidation of unreacted epoxide rings to form α-hydroxy aldehyde and carboxylic acid.[72] Degradation causes the epoxies to change from colorless to brown to cherry red with an accompanying increase in free-radical formation as monitored by electron paramagnetic resonance spectrometry[71]. Jain[73] first detected free-radical formation during thermo-oxidative degradation of epoxies. Ovenall[74], in more detailed studies of epoxies, concluded that at 180°C in air, the formation and decay of radicals occur by oxidative scission and molecular diffusion interaction between radicals, respectively. Later studies have suggested that resonance-stabilized free radicals occur in the thermal degradation of epoxies.[75,76] These data indicate that complex oxidative degradation reactions start to occur in DGEBA epoxies near 180°C and cause detectable embrittlement above ∿ 200°C. (Sorbed oxygen present in the epoxies allows such reactions to occur even when post-curing under vacuum.)

4.1.2 The TGDDM-DDS Epoxy System

Table 2 illustrates the percentage by weight of DDS required for (1) all primary and secondary amines in the DDS to react and (2) only primary amines to react with either 50 or 100% of the epoxide groups in the tetrafunctional TGDDM molecules.

TABLE 2 THEORETICAL REACTION MIXTURES FOR TGDDM-DDS EPOXY SYSTEM

	100% TGDDM Epoxide Groups React	50% TGDDM Epoxide Groups React
100% DDS primary and secondary amines react	37 wt% DDS	23 wt% DDS
100% DDS primary amines react	54 wt% DDS	37 wt% DDS

GP77-0731-36

Examination of molecular models indicates that considerable steric restrictions are present in the TGDDM molecule in the vicinity of the epoxide groups. Hence, because of this interference, it is unlikely that many secondary amines react in this system. Our studies indicate that steric and diffusional restrictions also limit the number of primary amines that react in the TGDDM-DDS system. Our cure conditions were 1 h at 150°C and 5 h at 177°C. The DDS is crystalline with a melting point of 162°C.

We have monitored the tensile mechanical properties of the TGDDM-DDS epoxy system as a function of composition (10-35 wt% DDS) and test temperature (23-250°C). Figure 9 is plot of tensile strength, ultimate elongation, and Young's modulus from 23-250°C for a TGDDM-DDS (35 wt% DDS) epoxy. The gradual decrease in tensile strength and modulus and the increase in ultimate elongation from 200-250°C suggests that a broad glass transition exists in this temperature range. Ultimate extension of $\geq$ 15% near T_g for epoxies with 15-35 wt% DDS suggests these glasses are not highly crosslinked.

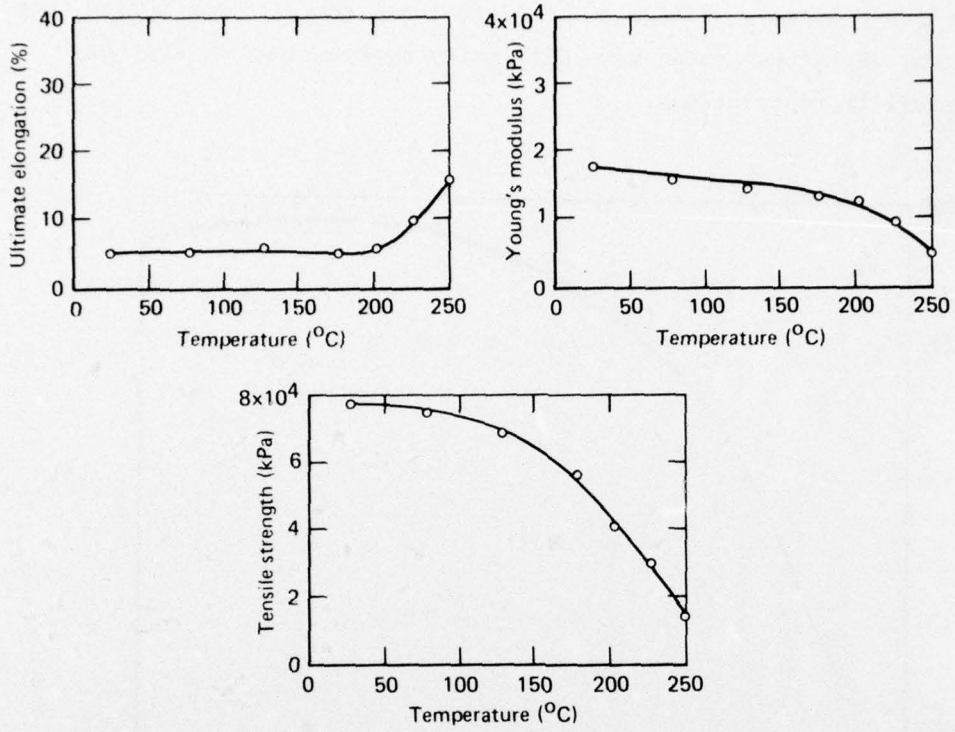

Figure 9 Tensile strength, ultimate elongation, and Young's modulus versus temperature for TGDDM-DDS (35 wt% DDS) epoxy that was deformed at a strain-rate of $\sim 10^{-2}$/min

A plot of T_g versus initial DDS concentration, shown in Figure 10, confirms that these epoxies are not highly crosslinked. [The temperatures representative of these broad T_g's were taken as those temperatures at which the room-temperature modulus (E_{RT}) decreased by half (i.e., $E_{RT}/2$)]. From 10-25 wt% DDS, the T_g rises with increasing DDS concentration because of corresponding increases in molecular weight and/or crosslink density. The T_g exhibits a maximum of $\sim$ 250°C at $\sim$ 30 wt% DDS and subsequently decreases for higher DDS concentrations. For epoxies prepared from > 25 wt% DDS, steric and diffusional restrictions evidently inhibit additional epoxy-amine reactions. Above $\sim$ 30 wt% DDS concentrations, unreacted DDS molecules plasticize the epoxy system and decrease the T_g. However, 37 wt% DDS is required to consume half the TGDDM epoxide groups when only epoxide-primary amine reactions occur (Table 2). Hence, the maximum in T_g at 30 wt% DDS suggests that less than half the TGDDM epoxide groups have reacted when 100% of the DDS is consumed. These observations illustrate that the 5 h, 177°C cured TGDDM-DDS epoxy systems are not

highly crosslinked because of steric and diffusional restrictions during cure. After gelation, unreacted groups have difficulty approaching one another because of mobility restrictions.

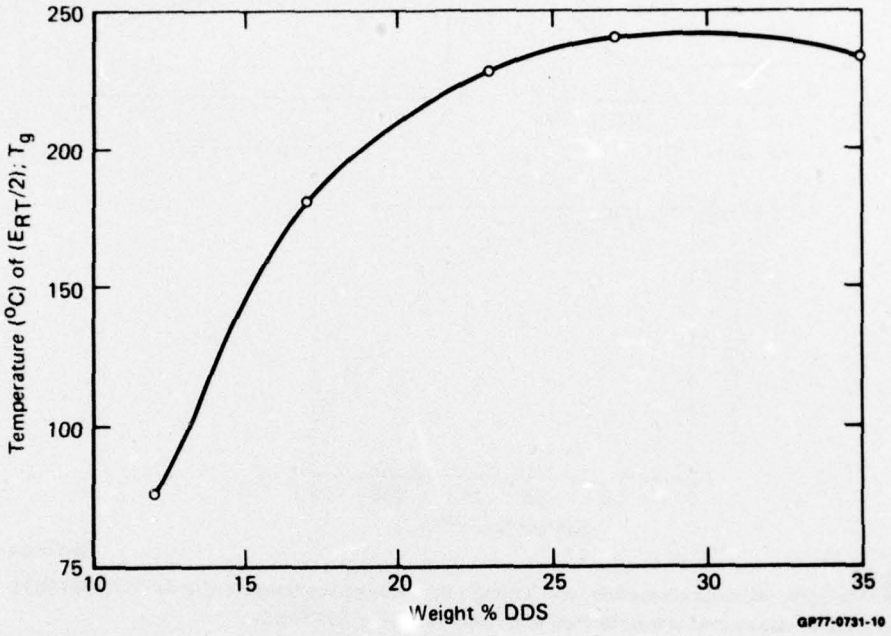

Figure 10 A measure of the T_g ($E_{RT}/2$) versus initial wt% of DDS in TGDDM-DDS epoxies

After cure, aggregates of unreacted DDS molecules have been detected in TGDDM-DDS ($\gtrsim$ 25 wt% DDS) epoxies by both electron diffraction and x-ray emission spectroscopy studies. Electron diffraction patterns were obtained from thin films prepared from $\gtrsim$ 25 wt% DDS that were similar to those obtained from the unreacted DDS crystals. The aggregates of unreacted DDS molecules crystallize after cooling the epoxy from its cure temperature. In addition, x-ray emission spectroscopy of fracture surfaces has detected regions of high sulfur content which are probably clusters of unreacted DDS molecules. In this technique, a fracture surface is bombarded with an electron beam, and the surfaces are scanned for emitted x-rays characteristic of sulfur. Figure 11 is an x-ray map of the sulfur distribution (indicated by the white dots) superimposed on the secondary scanning electron micrograph of the fracture surface. The large concentration of sulfur in the fracture-initiation region probably results from a cluster of unreacted DDS molecules.

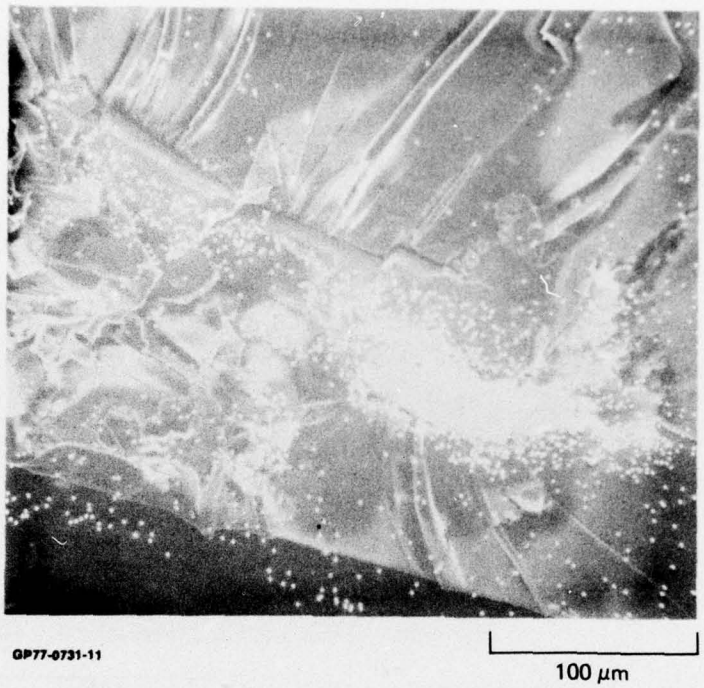

Figure 11 X-ray emission scanning spectroscopy map of sulfur distribution in the fracture surface of TGDDM-DDS (27 wt% DDS) epoxy which was fractured at 250°C

Bright-field transmission electron microscopy studies of the network structure of strained TGDDM-DDS epoxy films have revealed microscopic heterogeneities only in the brittle, low-molecular-weight systems prepared from 10-15 wt% DDS. In Figure 12(a), a strained TGDDM-DDS (10 wt% DDS) epoxy is shown to break into 2.5 to 13 nm diameter particles. At higher deformations, the network breaks into ∿ 2.5 nm diameter particles, as shown in Figure 12(b). These basic 2.5 nm diameter particles are of a similar size as the TGDDM molecule.

Evidence that the crosslinked network topography of TGDDM-DDS epoxies can be heterogeneous is suggested from fracture topography observations. Figure 13 shows scanning electron micrographs of the fracture topography initiation region of a TGDDM-DDS (23 wt% DDS) epoxy. Undeformed particles, 1-5 μm in size, are embedded in the deformed, surrounding material. These undeformed particles are possible regions of high-crosslink density which are embedded in a lower-crosslink density, deformable matrix.

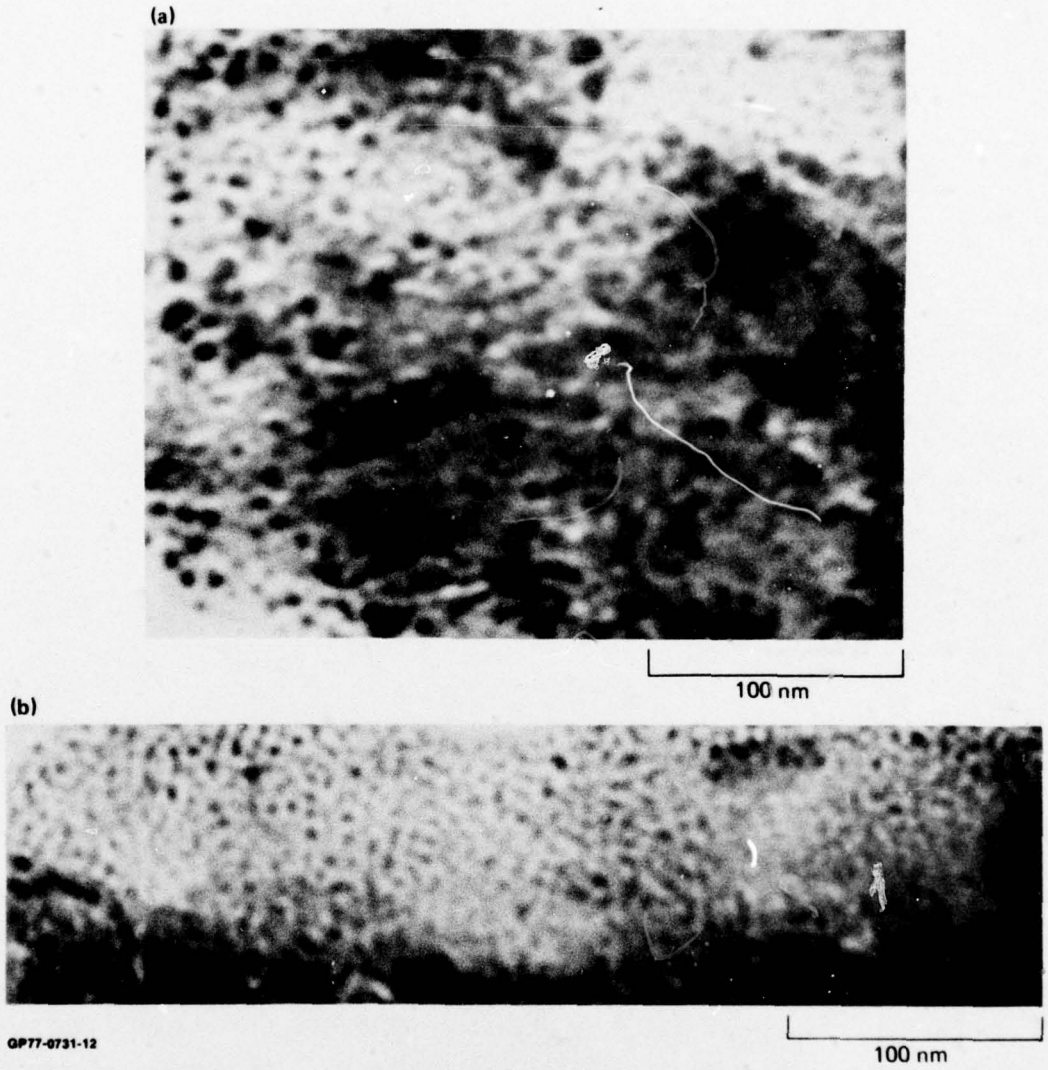

Figure 12 Bright-field transmission electron micrographs of structure in deformed TGDDM-DDS (10 wt% DDS) epoxy

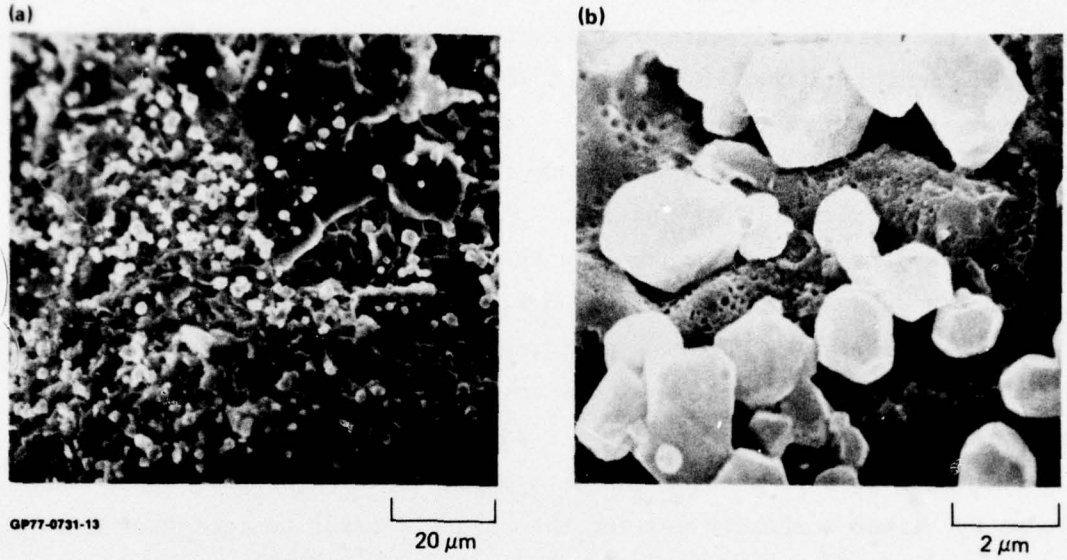

Figure 13 Scanning electron micrographs illustrating possible undeformed regions of high-crosslink density embedded in a lower-crosslinked density, deformable matrix in the fracture topography initiation region of a TGDDM-DDS (23 wt% DDS) epoxy, which was fractured in tension at room temperature at a strain-rate of $\sim 10^{-2}$/min

4.2 Microvoid Characteristics

Little attention has been given to the microvoid characteristics in thermosets, such as epoxies, and how such microvoids can be produced during fabrication. These microvoids can have a deleterious effect on the mechanical properties by acting as stress concentrators and also on the durability by serving as a sink for the accumulation of sorbed moisture. Microvoids can result in epoxies from (1) trapped air, which can be easily avoided if the appropriate precautions are taken during fabrication, and (2) low-molecular-weight material trapped in the glass which is subsequently eliminated during post-cure. This low-molecular-weight material results from either inhomogeneous mixing of epoxy monomer and curing agent and/or the inability of the constituents to react and resultant aggregation of these constituents.

4.2.1 The DGEBA-DETA Epoxy System

Pure DGEBA epoxy monomer crystallizes at room temperature (melting point 41.5°C) resulting in crystals that are suspended in the higher-molecular-weight liquid. In commercial DGEBA epoxides, such as Epon 828, the crystals are

$\sim$ 15 μm in size and predominantly in the form of square platelets, as illustrated in the optical micrograph in Figure 14. We have demonstrated for certain cure conditions that the presence of these crystallites can result in microvoids in the post-cured resin.[71] Partly curing the partially crystalline DGEBA epoxide monomer with DETA at room temperature leaves the crystals embedded in the glass. Post-curing $\geq$ 80°C under vacuum produces $\sim$ 10 μm microvoids and associated stresses in the epoxy as a result of melting the crystals and subsequent volatilization of the resultant liquid. Figure 15 illustrates the light-scattering patterns, under polarized light, associated with the microvoids and surrounding stress field in an amine-cured DGEBA system that was post-cured at 95°C for 24 h.

Such microvoid production can be avoided easily for DGEBA-based epoxy systems by either initially melting the crystals prior to curing or initially curing above the monomer crystalline melting point. These observations, however, do demonstrate that clusters of unreacted molecules present in an epoxy system during cure can, for certain cure conditions, result in microvoids in the finally cured glass.

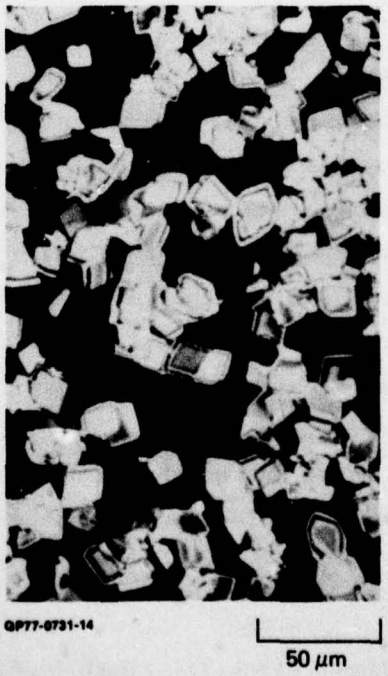

Figure 14 Optical micrograph of pure DGEBA crystals suspended in an unreacted commercial epoxide

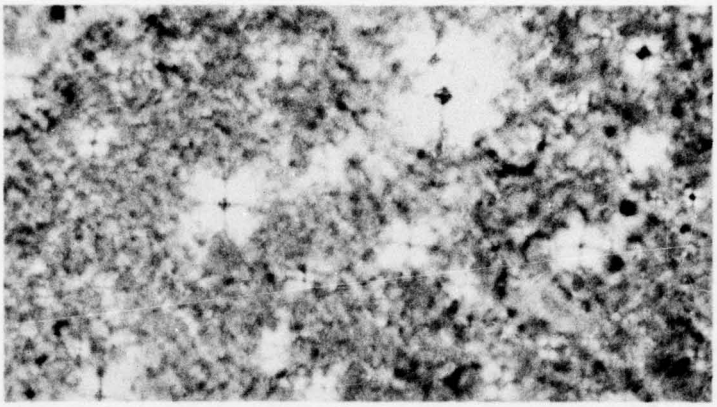

Figure 15 Light-scattering patterns, under polarized light, produced by microvoids and surrounding stress fields in an polyamide-cured DGEBA epoxy

4.2.2 The TGDDM-DDS Epoxy System

To obtain a TGDDM-DDS epoxy system with a high T_g, which is advantageous to limit the deleterious effects of sorbed moisture on this epoxy, requires ∿ 30 wt% DDS in the initial TGDDM-DDS mixture (see Figure 10). However, at these DDS concentrations, aggregates of unreacted DDS molecules can be present in the epoxy after the system forms a glass at the cure temperature. The elimination of these aggregates during subsequent cure could result in microvoids in the glass.

Microvoids are produced in the TGDDM-DDS system by elimination of unreacted, low-molecular-weight material. Figure 16 shows the progressive weight loss with increasing anneal temperatures from 150°-250°C for a TGDDM-DDS (27 wt% DDS) epoxy originally cured at 177°C for 5 h. In this figure, the amount of water subsequently sorbed by the epoxy at 120°C in an autoclave for 3 h is plotted versus anneal temperature. The increase in water sorption with increasing anneal temperature from 150°-200°C is associated with microvoids produced by volatilization of unreacted low-molecular-weight material. The water sorption exhibits a maximum in the 200°-225°C range and decreases as the anneal temperature approaches T_g at ∿ 250°C because the microvoids partially collapse.

Hence, a high T_g TGDDM-DDS epoxy system may contain microvoids which result from the elimination of aggregates of unreacted DDS molecules trapped in the glass during the early stages of cure.

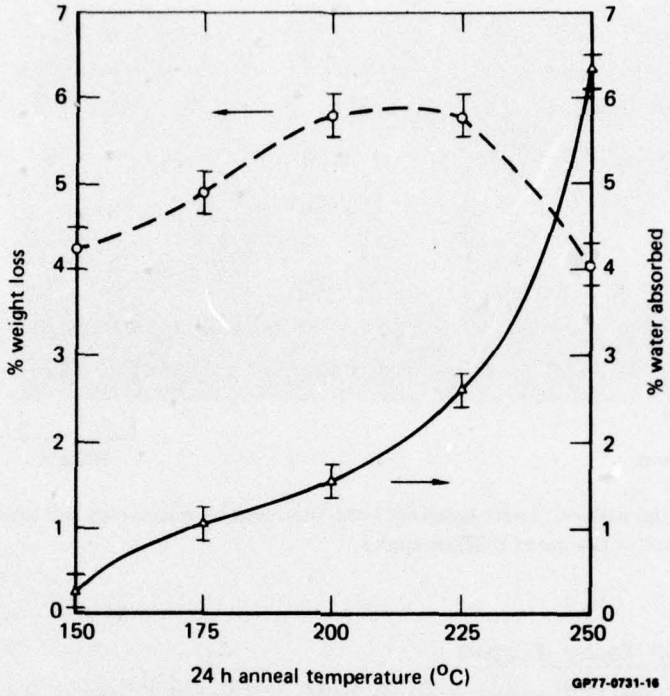

Figure 16 Plots of weight loss and subsequent water sorption versus anneal temperature for TGDDM-DDS (27 wt% DDS) epoxy

5. DEFORMATION AND FAILURE MODES OF EPOXIES

The relation between the network structure, microvoid characteristics, and failure processes of epoxies has received little attention. Localized plastic flow has been reported to occur during the failure processes of epoxies[53,55,71,77-84], and, in a number of cases, the fracture energies have been reported to be a factor of two to three times greater than the expected theoretical estimate for purely brittle fracture.[77,78,82,84-91] However, no systematic studies have been made to elucidate the microscopic flow processes that occur during the deformation of epoxies and the relation of such flow processes to the network structure.

Recently, we have conducted studies on the failure processes of amine-cured DGEBA epoxy systems and TGDDM-DDS epoxy systems. The major findings from these studies will now be reviewed.

5.1 The DGEBA-DETA Epoxy System

The failure processes of DGEBA-DETA epoxies were monitored by optical and electron microscopy of thin films deformed on a metal substrate and of the fracture topographies of epoxy specimens fractured in tension as a function of temperature and strain-rate. In addition, epoxy films were strained directly in the electron microscope, and the failure processes were monitored by bright-field microscopy. These studies indicate that epoxies fail by a crazing process.[83,92]

The structure of a craze is illustrated in Figure 17. Crazes only form in tension, and craze initiation involves cavitation at a stress concentration defect or inhomogeneity in the glass. Sternstein and Ongchin[93] have suggested that cavitation results from both the tensile dilatational component of the applied stress field and a normal yielding factor. This cavitation results in a highly porous structure at the craze tip. As the craze develops, microvoids formed by the cavitational craze-initiation process coalesce and enlarge, and polymeric material flows and orients in the direction of the applied tensile stress. This flow and orientation results, as illustrated in Figure 17, in fine, highly oriented fibrils within the well-developed craze. A crack will propagate through the craze when a cavity formed by enlargement and coalescence of microvoids attains a critical size and begins to propagate perpen-

dicularly to the tensile stress through the craze. The amount of energy expended in the form of viscous, molecular flow during the craze process is considerable and enhances the toughness of the material. Detailed discussions of the crazing and fracture processes of polymer glasses are given by Rabinowitz and Beardmore[12] and Kambour[94].

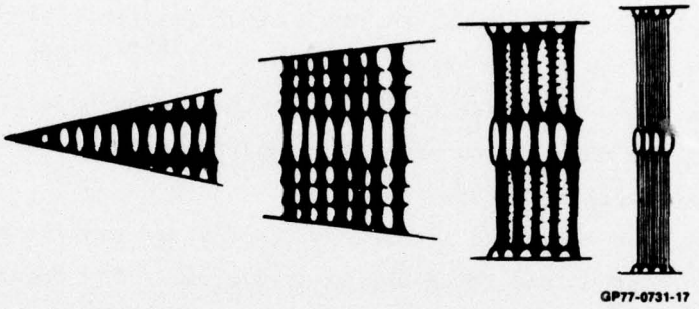

Figure 17 The structure of a craze

Crazes were observed in one-stage, carbon-platinum surface replicas of DGEBA-DETA epoxy films that were adhered to a brass substrate and strained $\sim$ 10% in tension. The replicas in Figure 18 illustrate the craze structure. The absence of any carbon-platinum particles within regions of the craze fibrils indicates that a thin epoxy layer adhered to the replica. At the craze tip, $\sim$ 10 nm diameter voids are produced by the tensile dilational stress fields [Figure 18(a)]. These voids coalesce to form larger voids $\lesssim$ 100 nm in diameter separated by 20-100 nm diameter fibrils. Further from the craze tip, the fibrils fracture as their length approaches $\sim$ 100 nm. The latter phenomenon may be a consequence of the poor structural integrity of the replica.

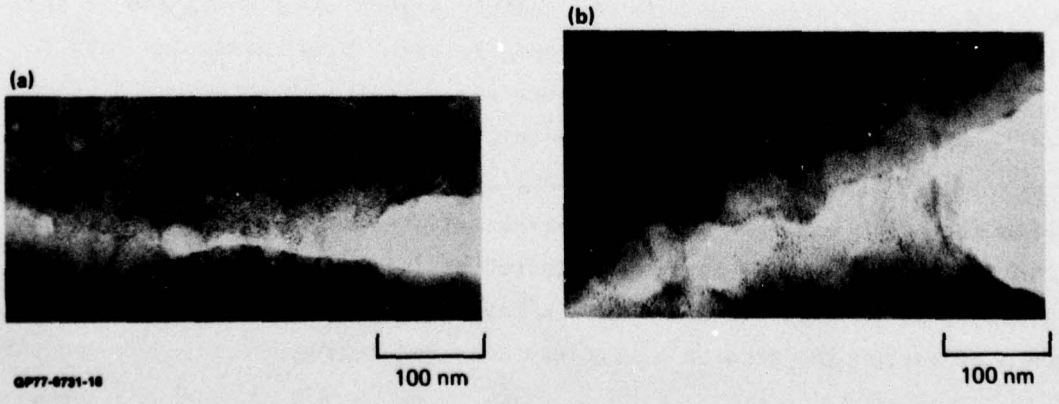

Figure 18 Carbon-platinum surface replicas of craze structure in DGEBA-DETA (11 wt% DETA) epoxy films that were strained on a metal substrate

Crazes were also found to propagate in ∿ 1 μm thick DGEBA-DETA epoxy films that were strained directly in the electron microscope. An overall view of a craze consisting of coarse 100-1000 nm wide fibrils is shown in the bright-field transmission electron micrograph in Figure 19(a). The region near the craze tip is shown in more detail in Figure 19(b). The structure of the coarse ∿ 1000 nm wide craze fibril shown in Figure 19(a) is illustrated in more detail in Figure 20. These micrographs reveal that the epoxy deforms inhomogeneously within the craze fibril [Figure 20(a)] and breaks up into 6-9 nm diameter particles. The network structure of 6-9 nm diameter particles within the region of the craze fibril is illustrated in Figure 20(b).

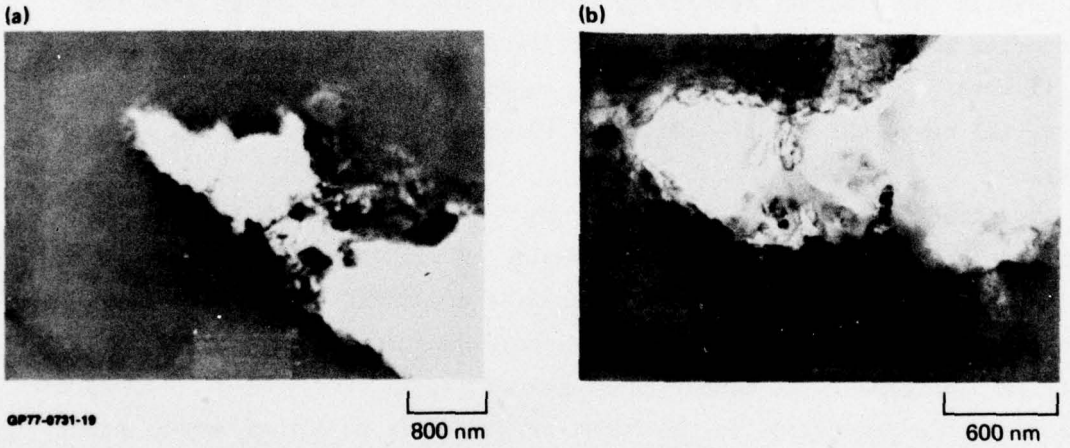

Figure 19 Bright-field transmission electron micrographs of (a) overall craze and (b) craze tip in DGEBA-DETA (13 wt% DETA) epoxy

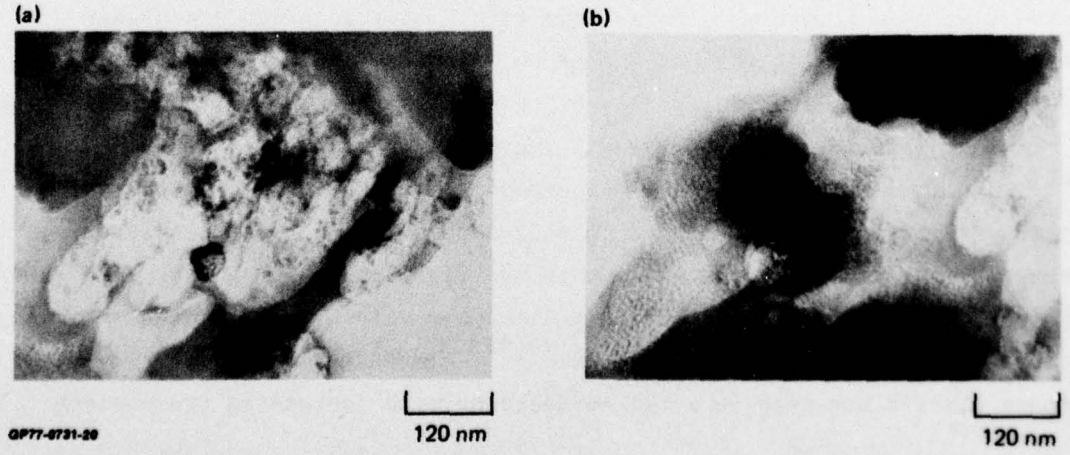

Figure 20 Bright-field transmission electron micrographs of craze fibril structure in DGEBA-DETA (13 wt% DETA) epoxy

The fracture topographies of DGEBA-DETA epoxies fractured as a function of temperature and strain-rate were studied by optical and scanning electron microscopy. The optical micrograph shown in Figure 21(a) illustrates the three characteristic topographic regions observed in these epoxies: (1) a coarse initiation region (dark area in the left of the micrograph), (2) a slow crack-growth, smooth, mirror-like region, and (3) a fast crack-growth, rough, parabola region. The topography varies with temperature and strain-rate, with the mirror-like region covering a larger portion of the fracture surface with increasing temperature and/or decreasing strain-rate, as illustrated in Figure 22.

The coarse initiation region often is found within a cavity as indicated by a cusp in the fracture topography which separates this region from the surrounding smooth, mirror-like region [Figure 21(b)]. The coarse structure can (1) cover a relatively small region in the center of the initiation cavity, (2) cover the entire cavity, or (3) irregularly cover parts of the cavity.

The structure of the coarse topography in the initiation region exhibited little consistency between samples or with varying temperature and strain-rate. A typical range of topographies consisted of the mica-like structure illustrated in Figure 21(c), a nodular structure and a collapsed fibrillar topography. At temperatures nearer the T_g (i.e., at T_g - 25°C) the fracture-initiation region in the DGEBA-DETA epoxies is either non-existent and/or much smoother than at lower fracture temperatures.

The fracture topography initiation region characteristics can be explained in terms of a crazing failure process. Murray and Hull[95] have reported that void growth and coalescence within a craze produce a planar cavity whose thickness is that of the craze. A mica-like structure in the slow crack-growth fracture topography of polymer glasses is generally associated with crack propagation through pre-existing craze material[96]. Murray and Hull[95] and Cornes and Haward[97] have observed irregularly furrowed or rumpled surfaces within initiation cavities in polystyrene and poly(vinyl chloride), respectively. Furthermore, there is evidence from studies on polystyrene that the initial stages of void growth and coalescence within a craze involve fracture through the center of the craze[98,99]. In addition, the coarseness of the craze fibrils has been reported to decrease with increasing craze width

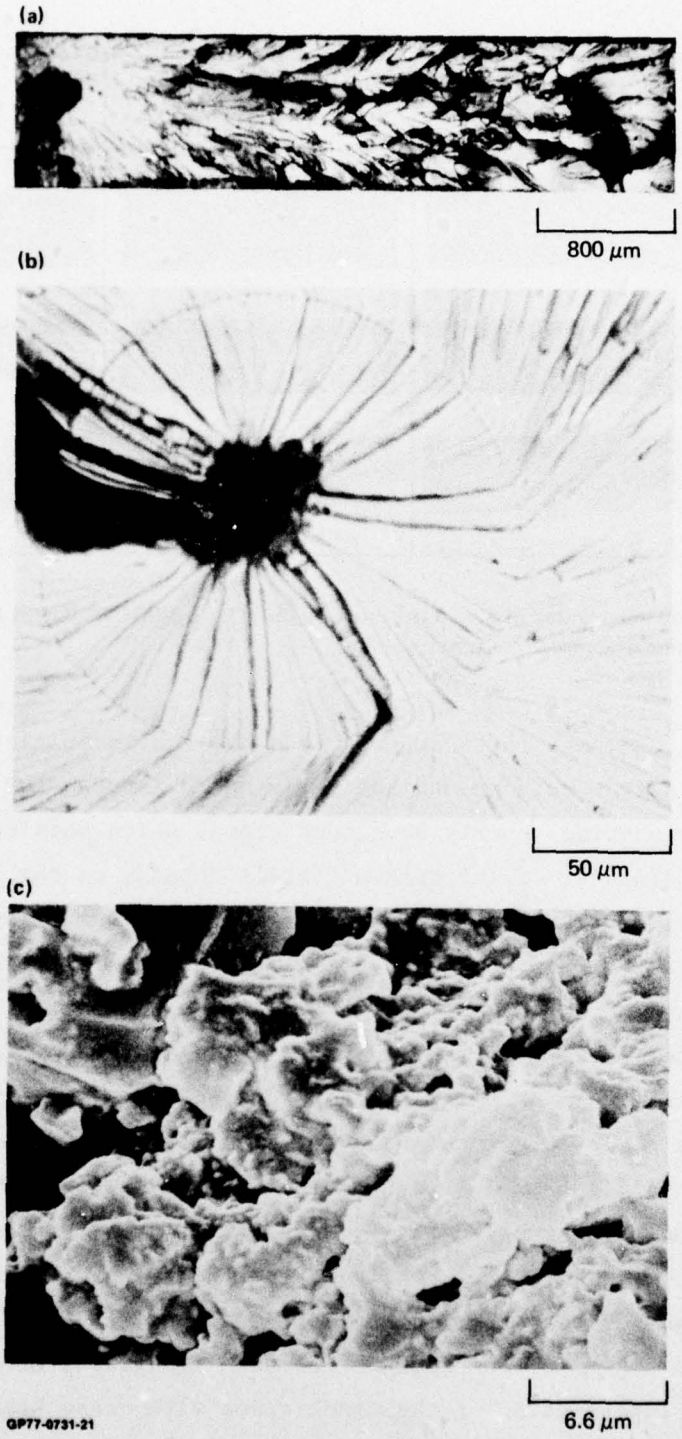

Figure 21 *Fracture topography of amine-cured DGEBA epoxies:* (a) optical micrograph of overall topography, (b) optical micrograph of slow crack-growth region, and (c) scanning electron micrograph of initiation region

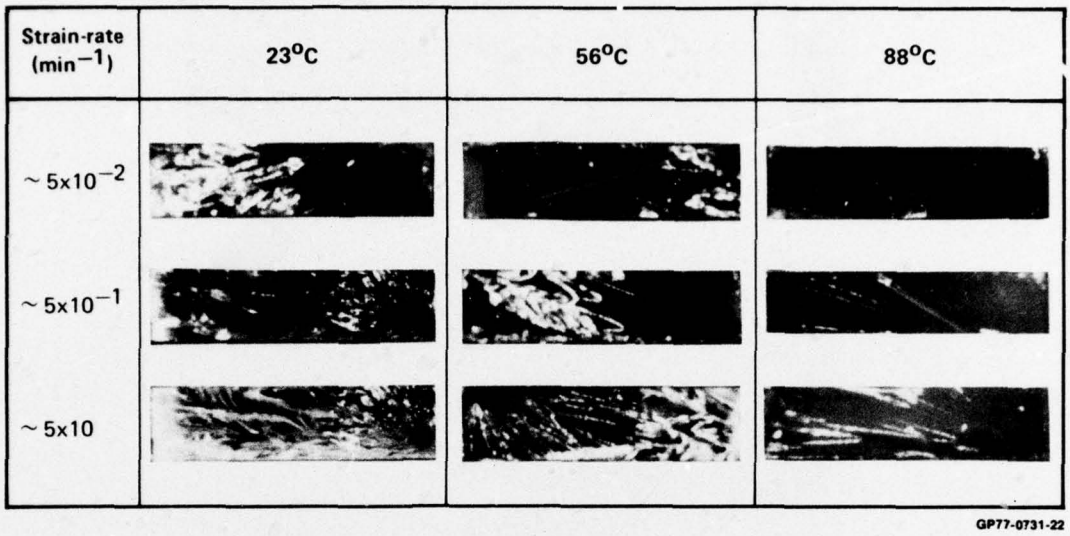

Figure 22 **Optical micrographs of overall fracture surfaces of DGEBA-DETA (9 wt% DETA) epoxies as a function of temperature and strain-rate**

and thickness[99]. These facts suggest that the coarse initiation region in epoxies results from void growth and coalescence through the center of a simultaneously growing, poorly developed craze, which consists of coarse fibrils. The diameter of the broken fibrils depends on the relative rates of craze and void growth. Nodular particles and fibrillar structures that lie parallel to the fracture surface are associated with fractured craze fibrils. Doyle[100,101] and Hoare and Hull[102] have reported broken fibrils that lie parallel to the fracture surface in polystyrene and have suggested that these fibrils are swept down onto the fracture surface as the crack passes through the craze. We cannot preclude, however, that the mica-like structure such as that observed in Figure 21(c) results from the coalescence of a bundle of parallel microcrazes situated in slightly different planes rather than directly from the fracture of poorly formed, coarse craze fibrils. Skibo et al.[103] suggested that the mica-like structure which they observed in the non-initiation region of the fatigue-fracture topography of polystyrene is a result of the intersection of the crack plane with craze bundles. The more nodular-like topographies are similar to those observed in the fracture topographies of certain multi-phase metals[104] and polyvinyl chloride[105-107]. In polyvinyl chloride, this structure has been associated with particulates in the polymer resulting from imperfect melting of resin particles.[105-107]

Hence, we also cannot preclude that any heterogeneity in the epoxy structure could be partially responsible for the observed topographies.

The variation in the fracture topography initiation region which did not exhibit consistent trends with strain-rate and temperature, except for the disappearance or smoothening of the coarse topographies in those specimens fractured near T_g, is a result of a number of factors: (1) the relative rates of crack and craze propagation, (2) the craze structure immediately prior to crack propagation through the craze, (3) the modification of the craze structure by crack propagation, (4) the collapsing and relaxation of the craze remnants after crack propagation, and (5) the variation in the local stress fields in the vicinity of the growing craze or crack which depend on the microvoid characteristics of the epoxy.

The smooth mirror-like region of the fracture topography of DGEBA-DETA epoxies whose area increases with increasing temperature and decreasing strain-rate (Figure 22) can be attributed to a crazing process. For other polymers, this region has been associated with slow crack-growth, and its size varies with temperature, molecular weight and strain-rate.[108-111] In studies on polyester resins, Owen and Rose[112] report that the mirror-like area increases with resin flexibility. A number of workers have associated this smooth fracture topography region with slow crack-propagation through the median of the craze with subseqent relaxation of craze remnants.[95,96,101,102,113,114] El-Hakeem et al.[114] have directly observed the masking of the microfeatures of this fracture topography region by the subsequent relaxation processes. The smoothness of the fracture topography region surrounding the coarse initiation region in DGEBA-DETA epoxies results from crack propagation either through the center or along the craze-matrix boundary interface of a thick, well-developed craze consisting of fine fibrils. The presence of fine fibrils would produce a smoother fracture topography than in the coarse initiation region, irrespective of any subsequent relaxation of craze remnants. One-stage, carbon-platinum surface replicas of the mirror-like region reveal areas consisting of 15-30 nm diameter particles. This granular appearance of the replica could be the result of fractured fine fibrils aligned normal to the surface. However, we cannot preclude that such structures are regions of high-crosslink density. The extent of the mirror-like region is a measure of the area in which crack propagation occurs through a preformed craze.[95] For a fracture surface completely covered by the mirror-like region, crazes have

grown completely across the specimen prior to any significant crack propagation.[102] Hoare and Hull[102] have suggested that this area depends on (1) the ease of cavitation and crack propagation within the craze, (2) the rate of craze nucleation and growth, and (3) the concentration of crazes. The decrease in the crazing stress with increasing temperature and/or decreasing strain-rate favors craze growth, which will result in a larger mirror-like region.

River markings which radiate from the fracture-initiation site are also observed in the mirror-like region, as illustrated in Figure 21(b). These markings, which vary inconsistently between epoxy specimens, are steps formed by the subdivision of the main crack into segments running on parallel planes. This subdivision could result from the interaction of the crack front with the craze structure. Owen and Rose[112] have found that the river markings become ordered and regular as the flexibility and therefore the ability to undergo crazing in polyester resins is enhanced.

Interference colors, often observed in the mirror-like region of non-crosslinked polymer glasses[6], were not evident in the fracture topography of DGEBA-DETA epoxies. Broutman and McGarry[77] also found that interference colors were absent in the fracture surfaces of crosslinked polymethylmethacrylates. They suggested that the thickness of the craze or craze remnants in the mirror-like regions of these crosslinked glasses was not large enough to cause interference with visible light. A similar explanation may apply to epoxies where the presence of crosslinking presumably inhibits the development of thick crazes.

5.2 The TGDDM-DDS Epoxy System

TGDDM-DDS epoxies exhibit fracture topography characteristics similar to those of the DGEBA-DETA epoxies, which indicates that they too deform and fail primarily by a crazing process. The fracture topography initiation region characteristics of a TGDDM-DDS (27 wt% DDS) epoxy are illustrated in Figure 23. The overall fracture topography initiation cavity is illustrated in Figure 23(a); 1-5 μm diameter, poorly developed, fractured fibrils are shown in Figure 23(b), and well-developed, 100-200 nm diameter finer fractured fibrils are illustrated in Figure 23(c). The size distribution of the fractured fibrils within the initiation region depends on the relative rates of craze and crack propagation (see Section 5.1). Elongated fibrils that were

swept onto the fracture surface were found in the TGDDM-DDS epoxy fracture topographies as illustrated in Figure 24.

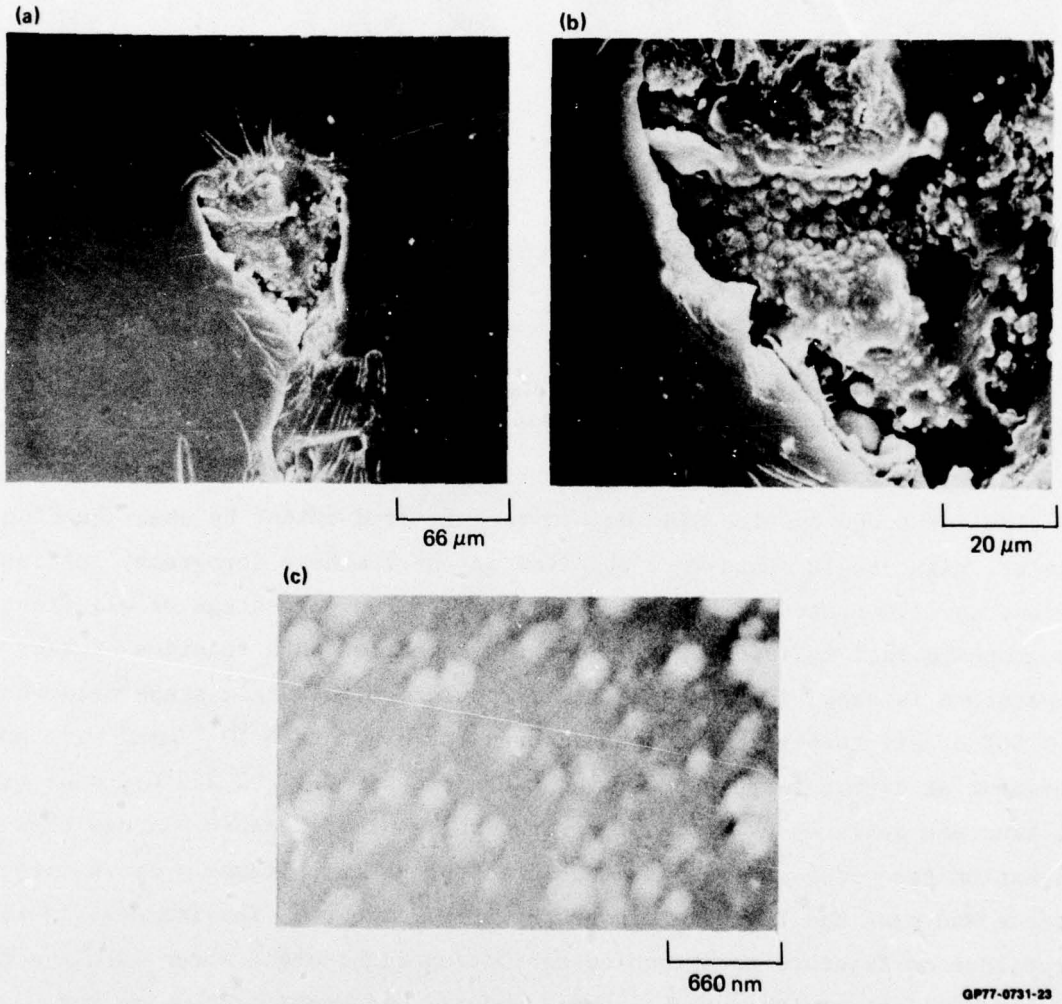

Figure 23 Scanning electron micrographs of (a) overall fracture topography initiation cavity, (b) coarse fractured fibrils, and (c) fine fractured fibrils in TGDDM-DDS (27 wt% DDS) epoxy, fractured at room temperature at a strain-rate of 10^{-2}/min

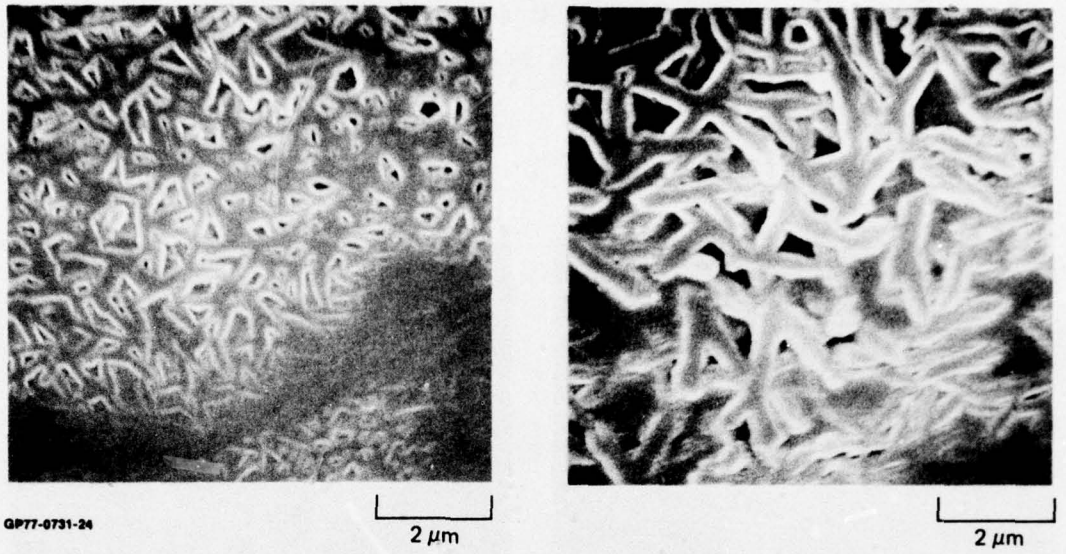

Figure 24 Scanning electron micrographs of fibrils swept onto the fracture surface in TGDDM-DDS (23 wt% DDS) epoxy, fractured at 200°C at strain-rate of 10^{-2}/min

The TGDDM-DDS epoxies also deform to a limited extent by shear banding.[115] Regular, right-angle steps were observed in the fracture topography initiation region, as illustrated in Figure 25. A plot of the percentage of all fracture topographies that exhibited this mode of deformation as a function of test temperature is shown in Figure 26. The regular, right-angle steps observed in ∿ 20% of all room-temperature fractures (strain rate ∿ 10^{-2}/min) were more prevalent at higher temperatures. At and above 250°C ($T_g \tilde{\sim} 250$°C), none of the fracture surfaces exhibited the right-angle steps because viscous flow and relaxation processes during and after crack propagation cause a smooth fracture surface and mask the fracture topography microfeatures. The increase in the percentage of fracture topographies exhibiting right-angle steps with temperature is consistent with the shear-band mode of deformation becoming more favored relative to the crazing mode with increasing temperature.[21,93,116] Shear-band propagation in these crosslinked glasses produces structurally weak planes because of bond cleavage caused during molecular flow. Hull[117] and Mills[118] have both noted that the intersection of shear bands, which occurs at right angles, causes a stress concentration. This stress concentration is sufficient to cause a crack to propagate through the structurally weak planes caused by shear-band propagation. These phenomena produce right-angle steps in the fracture topography.

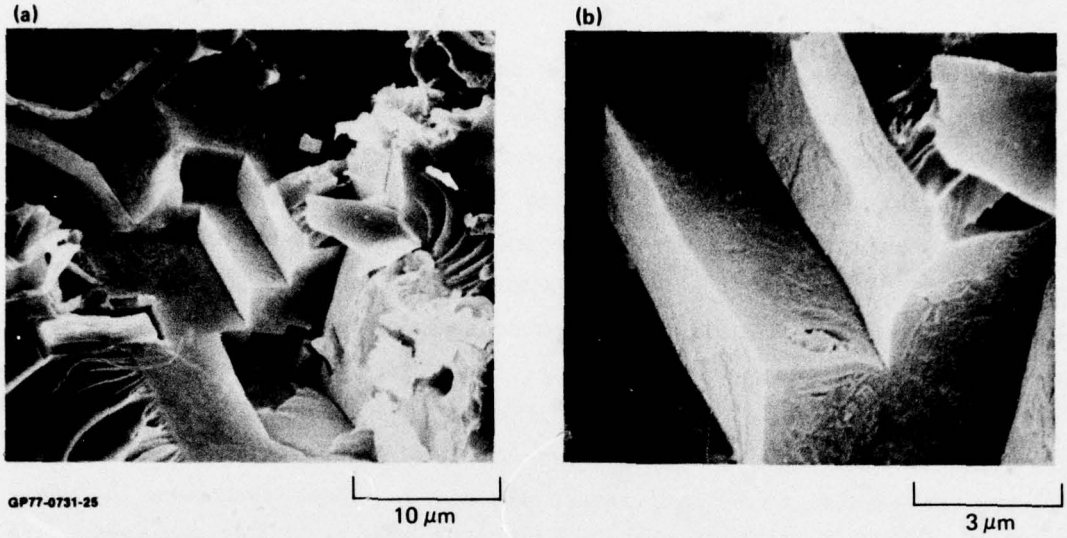

Figure 25 *Scanning electron micrographs of right-angle steps in the fracture topography initiation region of* TGDDM-DDS (35 wt% DDS) epoxy fractured at 225°C at a strain-rate of 10^{-2}/min

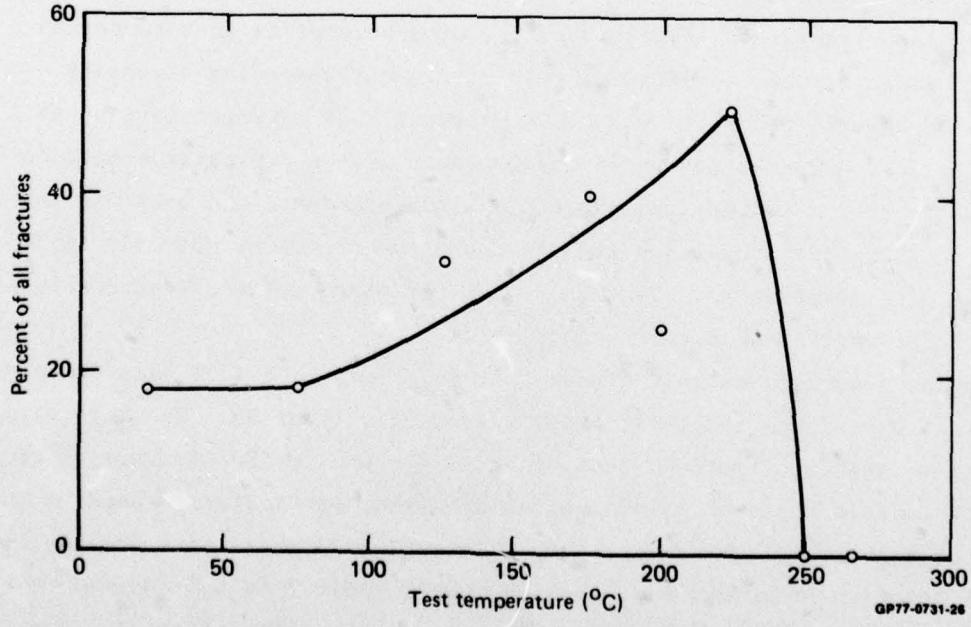

Figure 26 Percentage of fracture topography initiation regions that exhibit right-angle steps versus temperature in TGDDM-DDS (15-35 wt% DDS) epoxies

6. EFFECTS OF SORBED MOISTURE ON DURABILITY OF EPOXIES

Epoxy composites and adhesives sorb moisture which in both laboratory and field tests deteriorates the mechanical properties, particularly at high temperatures. The effect of sorbed moisture on the physical properties and mechanical integrity of epoxies and other thermosets utilized as adhesives and composite matrices in the aerospace industry has received considerable attention.[1,2,19,82,84,86,88,119-179] Despite these studies, all the basic mechanisms responsible for moisture-induced degradation of epoxies have not been identified and/or understood; hence, the durability of epoxy components in the service environment is still uncertain. In this section, the pertinent basic physical phenomena induced and/or modified by sorbed moisture and affecting the durability of epoxies are discussed. These phenomena include (1) lowering of T_g by sorbed moisture, (2) diffusion of sorbed moisture, (3) swelling stresses induced by sorbed moisture, (4) modification of the deformation and failure modes and the mechanical response by sorbed moisture, and (5) interaction of sorbed moisture with other environmental factors.

6.1 The Glass Transition

The glass transition temperature, T_g, of a polymer is that temperature at which the glass becomes a viscous liquid with a corresponding viscosity decrease of several orders of magnitude within a $\sim$ 10 K temperature range. This transition is a second-order phase change and unlike a crystalline melting point occurs over a temperature range, is time dependent, and does not involve changes in extensive properties such as enthalpy and volume but only their rates of change with temperature. Near T_g, a polymer glass softens with decreases in tensile strength and increases in ductility.

Epoxies generally exhibit broad, T_g's (see Section 4.1.2) because of the presence of crosslinks and their heterogeneous distribution. The large-scale, cooperative segmental motions that occur at T_g require the cleavage of crosslinks for certain types of morphological networks, particularly those in which regions of high-crosslink density form the continuous phase (see Section 4.1).

The sorption of moisture by epoxies lowers their T_g's and correspondingly causes them to soften at lower temperatures. The lowering of the T_g by a diluent, plasticization, is a result of a decrease in the free volume (total volume minus molar volume) of the system caused by the addition of the lower

free-volume diluent. The free volume at T_g for a wide variety of glass-forming materials has been shown to be a constant and have a critical free-volume fraction of 0.025 of the total volume.[180-182] Kelley and Bueche[183] have derived an expression relating the T_g of a polymer-diluent system to that of the T_g's of the two components. The Kelley-Bueche equation assumes that the free volume contributed by the diluent is additive to that of the polymer and that the free volumes of the mixture and components at their T_g's are a universal constant. The Kelley-Bueche equation for the T_g of the polymer-diluent system is

$$T_g = \frac{\alpha_p V_p T_{gp} + \alpha_d (1 - V_p) T_{gd}}{\alpha_p V_p + \alpha_d (1 - V_p)}, \qquad (1)$$

where T_{gp} = T_g of the polymer

T_{gd} = T_g of the diluent,

α_p = coefficient of expansion of polymer

α_d = coefficient of expansion of diluent, and

V_p = volume fraction of the polymer.

For an epoxy-water system, the Kelley-Beuche equation must be used in a simplified form. The coefficient of expansion of amorphous water between its T_g and melting point (T_M) at 0°C is unknown. Therefore, assuming $\alpha_p \simeq \alpha_d$, the Kelley-Beuche equation simplifies to

$$T_g = V_p T_{gp} + (1 - V_p) T_{gd}. \qquad (2)$$

Experimentally, the T_g of water has been reported in the 128-142 K range.[184-189] A good empirical rule[190] for most substances is

$$T_g/T_M \simeq 1/2 \text{ to } 2/3, \qquad (3)$$

which places the T_g of water in the 137-182 K range. In Figure 27, we compare Browning's[177] experimentally determined T_g's of a BF_3:NH_2-C_2H_5 catalyzed TGDDM-DDS epoxy-moisture system, which contains equilibrium amounts of sorbed moisture, with the theoretically calculated values of T_g determined from Equation (2). The upper limits of the theoretical plot are calculated assuming a T_g of water of 182 K, whereas the lower limits are determined utilizing a T_g of 135 K. The experimental data points are well below the theoretical predictions. This discrepancy could be caused by the following phenomena: (1) the strong hydrogen-bonding capability of water could produce anomalous effects or (2) if the epoxy has a heterogeneous-crosslink density distribution, moisture will preferentially sorb in the regions of low-crosslink density. The regions of low-crosslink density control the flow processes that occur at T_g. Equilibrium moisture gains are determined by assuming a uniform moisture distribution. However, a non-uniform distribution could lead to local moisture concentrations in low-crosslink density regions that are considerably greater than those implied for a uniform moisture distribution. Hence, the depression of T_g may be greater than that expected for a homogeneous distribution of sorbed water. Therefore, the depression of T_g of TGDDM-DDS epoxies by sorbed moisture is considerably greater than that predicted theoretically.

The plasticization of epoxies by sorbed moisture has generally been reported to be reversible since desorption of moisture from the polymer regenerates the original physical and mechanical properties.[1,2,19,82,84,86,88,119-179] However, in many environments, irreversible, permanent-damage regions can easily be produced in epoxies during the moisture sorption and desorption processes. These phenomena will be discussed in later sections.

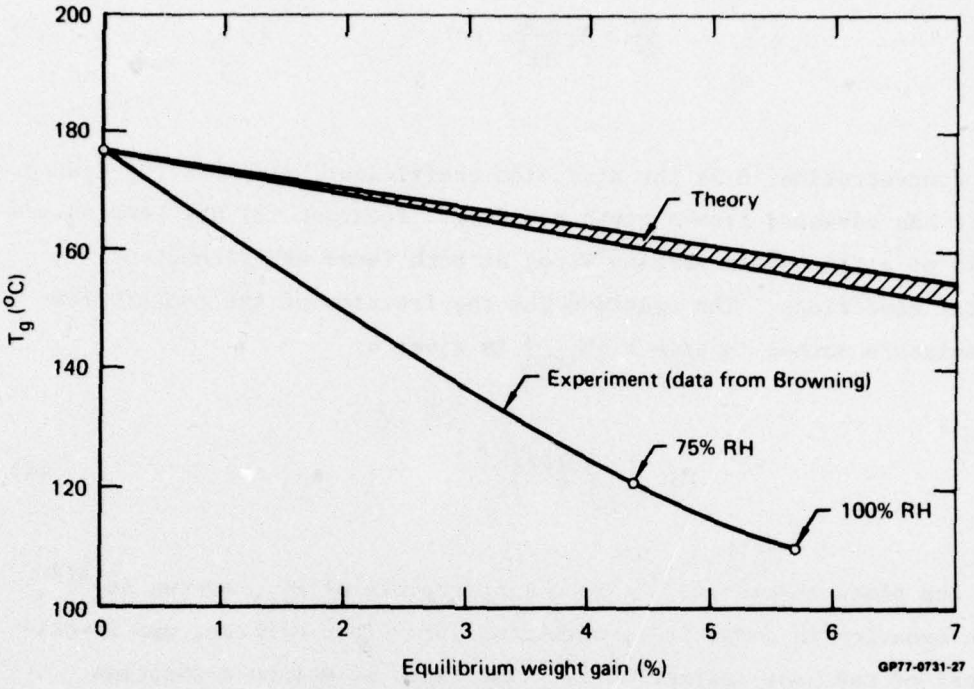

Figure 27 Theoretical and experimental plots of T_g vs equilibrium moisture weight gain for BF_3:NH_2–C_2H_5 catalyzed TGDDM-DDS (24 wt% DDS) epoxy-moisture system

6.2 Diffusion

The durability of epoxies in many aerospace service environments depends on the degree of deterioration of the high-temperature mechanical properties caused by the plasticizing effect of sorbed moisture and whether this phenomenon is adequately considered during the design stage. The previous relative-humidity time-temperature exposure of the epoxy component and the diffusion characteristics of moisture in this component determine the moisture profile and the resultant mechanical response of the material. Hence, the diffusion characteristics of moisture in an epoxy component are critical factors for predicting mechanical response and durability in a given service environment.

Many diffusion processes can be adequately described by Fick's laws of diffusion.[191] A number of workers have successfully applied Fick's second law of diffusion to the sorption and desorption of moisture in epoxies and epoxy composites and have predicted the moisture profiles as a function of time for specific environmental conditions.[1,2,156,158,165,166,167,169,175,177,178] Fick's second law for one-dimensional diffusion is given by

$$\frac{dc}{dt} = D \frac{d^2c}{dx^2} \quad , \tag{3}$$

where c is concentration, D is the diffusion coefficient, and x is the distance the moisture has advanced from a given boundary. Equation (3) has been solved for the case of a flat sheet sorbing vapor at both faces under constant environmental conditions. The solution for the fraction of the equilibrium amount of moisture sorbed in time t [$M_{(t)}$] is given by

$$M_{(t)} = \frac{4}{l} \left(\frac{Dt}{\pi}\right)^{1/2} \quad , \tag{4}$$

where l is the plate thickness.[192] From linear plots of $M_{(t)}$ versus $(t)^{1/2}$, the Fickian behavior in composites, corrected for volume effects, was identical with that of the neat resins.[156,158] The rates of moisture sorption increased with temperature, and the equilibrium amount of moisture was directly proportional to the relative humidity.

At high moisture contents [$M_{(t)} \geq 0.6$], Equation (4) does not hold, and a number of methods have been used to determine the moisture profiles in epoxies and epoxy composites. Estimates within 15% of the moisture content and its distribution have been obtained from a series solution of Equation (3) by Shen and Springer[169] and from a hyperbolic tangent method developed by McKague[168]. Bohlmann and Derby[178] have noted that a numerical-methods technique utilizing a computer program[193] must be used to account for the moisture profile for transient conditions with different relative humidities at each surface.

The utilization of Fickian diffusion as the controlling mechanism to predict the concentration and distribution of sorbed moisture and corresponding deterioration in the high-temperature mechanical properties can lead to serious errors in the durability predictions of epoxies in many environments. Any damage induced in the epoxy or epoxy composite by fabrication and/or environmental conditions can cause deviations from Fickian diffusion and accelerate moisture sorption.

Non-Fickian diffusion has been observed in polymers[194] in which the diffusion coefficient also becomes time and concentration dependent. This type

of diffusion has generally been attributed to interaction between the polymer and penetrant[195-202], voids in the polymer[203-207], and clustering of the penetrant in the polymer[194,208-212].

Non-Fickian diffusion of moisture in epoxies and epoxy composites generally results from the perturbation of the diffusion processes by microvoids and/or cracks. These voids or cracks can be caused by many factors such as one or a combination of the following phenomena: (1) swelling stresses induced by the sorbed moisture (see Section 6.3), (2) craze cavitation (see Section 6.4), (3) formation of water clusters and their subsequent elimination from the glass (see Section 6.5), and (4) high surface tensile stresses resulting from temperature and moisture gradients (see Section 6.5).

Sorbed moisture can modify the epoxy network and therefore the moisture diffusion characteristics in that network. These network modifications can be (1) bond cleavage as a result of swelling stresses[179] and/or relaxation of fabrication stresses, (2) formation of additicnal crosslinks by moisture-enhanced mobility of unreacted groups, and (3) modification of the free volume and/or microvoid characteristics.

In epoxy composites, anomalous diffusion can also occur as a result of (1) accelerated diffusion along the fiber-matrix boundary interface because the presence of voids at the interface creates a preferential diffusion path[175] and (2) stress-biased diffusion caused by anisotropic swelling stresses in the composite[213].

Hence, a number of phenomena, some of which have been alluded to in this section and will be discussed in greater depth in subsequent sections, can cause non-Fickian diffusion of moisture in epoxies and epoxy composites. This non-Fickian diffusion, if not considered during the design stage of an epoxy component, can seriously modify the durability in many long-term applications.

6.3 Swelling

Sorbed moisture causes epoxies to swell.[1,175,177] The swelling stresses generated by the sorbed moisture can significantly affect the durability of epoxies in many environments. Swelling stresses caused by moisture gradients, together with other stresses inherent in the material, such as fabrication stresses, can be sufficiently large to cause localized fracture of the polymer[177] (see Section 6.5). For example, the crazing of polystyrene on sorption of normal hydrocarbons has been shown to result from a coupling of the

relaxation of orientation stresses frozen into the glass and the swelling stresses which are produced at the boundary between the swollen, outer regions of the glass and the unswollen core.[124-218] Furthermore, Fourier-transform infrared spectroscopy suggests that the swelling stresses are sufficient to cleave bonds in the crosslinked, TGDDM-DDS epoxy system.[179] Although the moisture-induced swelling of epoxies generally results in only a 1-2% thickness increase, these dimensional changes can result in high stresses in a composite where the fibers constrain the swelling.

For durability predictions of epoxies, the local magnitude of the swelling stresses and strains and at what stress or strain they produce permanent damage in the epoxy glass must be known. Halpin[175] has calculated the dilatational strains in epoxies assuming volume additivity and a homogeneous water distribution. However, the experimentally observed swelling strains were greater than predicted by theory by a factor of three at moisture contents $\lesssim$ 2%. The swelling of elastomers by diluents can be adequately treated by kinetic theory of rubber elasticity utilizing Gaussian statistics.[67,219,220] However, the swelling of a non-uniform, high-crosslink density epoxy glass is considerably more difficult to treat on a fundamental level. Gaussian statistics cannot be utilized at high-crosslink densities. Also, a heterogeneous-crosslink density distribution could produce non-uniform diffusion at low concentrations as has been suggested for other heterogeneous systems.[221-225] In these systems, some of the penetrant molecules are envisaged to diffuse faster along certain unspecified paths.

To compute the moisture sorption levels for specific environmental conditions that cause network modification and subsequent growth of permanent damage regions in epoxies requires (1) further experimental and theoretical studies on moisture-induced swelling stresses and strains and (2) a detailed knowledge of the network structure and the stress levels in the presence of moisture at which damage occurs in the network (see Section 6.4).

6.4 Modes of Deformation and Failure and Mechanical Response

In Section 5, evidence was presented to show that crazing is the predominant mode of deformation and failure in the TGDDM-DDS and DGEBA-DETA epoxy systems. In any durability prediction, it is vital to understand how sorbed moisture modfies the crazing process and mechanical response. Sorbed

low-molecular-weight liquids generally cause failure in polymers by inducing crazing or cracking at stresses much lower than those observed in their absence. Numerous studies[22,82,84,86,88,94,170-172,211,214-218,225-269] on the interaction of low-molecular-weight diluent molecules on the crazing process have illustrated that this phenomenon is complex and not completely understood on a molecular level. This section reviews the basic physical phenomena responsible for modification of the crazing process in the presence of low-molecular-weight diluent molecules, presents evidence that sorbed moisture modifies the crazing process and mechanical response of TGDDM-DDS epoxies, and discusses the implications of these findings in relation to the durability of TGDDM-DDS epoxies.

The modification of craze initiation and propagation by the presence of diluents can occur as a result of plasticization[227] and/or surface energy reduction[234]. The presence of the diluent at the craze tip can reduce the surface energy of the polymer, facilitating the creation of a new surface.[263] For an sorbed diluent layer at least a few molecules thick, the interfacial surface energy participating in craze cavitation can be reduced from the higher polymer-air surface energy value. The plasticization of the polymer at the craze tip by the diluent lowers the shear yield stress which is also active in the craze cavitation process. The stress concentration at the craze tip increases the fractional free volume of the polymer which both enhances sorption of the diluent and lowers the T_g of the polymer.[22,263]

Andrews and coworkers[231,244,249] have shown that solvent craze formation (W) is governed by the cavitation properties of a solvated zone of polymer at the craze tip:

$$W = 4.84\ (h\gamma/p)\ f^{2/3} + 0.66\ Y\psi hf \qquad (5)$$

where h is the craze thickness, γ the interfacial energy of the voids, p the mean distance between the void centers, f the void fraction, Y the shear yield stress, and ψ a constant with a value of 4.4. These threshold conditions for craze cavitation depend on the work necessary to produce plastic yielding and the work necessary to create void interfaces. The yield stress is strongly temperature dependent relative to the surface energy term. Andrews and coworkers showed that W decreases with temperature and that, above a critical

temperature T_c, W assumes a minimum constant value W_o. The temperature T_c has been associated with the T_g of the plasticized swollen polymer at the craze tip. The yield stress term in Equation (1) reduces to near zero at T_g because $Y \simeq 0$ at or above T_g. When $Y \simeq 0$, W is dependent only on the temperatue-dependent surface energy term.

More recently, Kambour and coworkers[250] have suggested that the plasticization effect is the more important factor in solvent-crazing. They reported that the solvent-crazing resistance of undiluted polystyrene is the same as that of the preplasticized polystyrene in air. This finding implies that the presence of a liquid/polymer interface is not critical to crazing effectiveness of a given diluent. These workers, therefore, concluded that liquids do not appear to reduce crazing resistance by flowing into and wetting the surface of holes as they form.

There have been a number of efforts to correlate the modification of the craze-crack behavior of the polymer in the presence of a diluent with the solubility parameters of the polymer and diluent. Bernier and Kambour[233] studied the effect of a variety of liquids on the failure of poly(2,6-dimethyl-1,4-phenylene oxide). They concluded that a liquid acts as a solvent when its solubility parameter is close to that of the polymer. When the difference between the solubility parameters of the liquid and polymer is small, the liquid promotes cracking; when this difference is large, crazing is enhanced. Vincent and Raha[240], however, found that a more effective representation of the solvent-cracking versus crazing behavior is obtained by considering the capacity of each liquid-to-hydrogen bond in addition to its solubility parameter.

Kambour and coworkers[233,239] have also shown a close correlation between the critical strain for craze or crack formation (e_c) and the solubility parameter of the diluent. Subsequently, Andrews and Bevan[244] found that the work of solvent craze formation (W) above the T_g of the plasticized polymer at the craze tip, is a smooth function of the difference in the solubility parameters of the polymer (δ_p) and the diluent (δ_d), ($\delta_p - \delta_d$). These workers also found that W exhibits a minimum at $\delta_p \simeq \delta_d$. More recently, Mai[269] has reported that W,δ_d relations are not affected by hydrogen bonding. Despite these reported correlations between the solubility parameters of polymer and diluent and the work of craze cavitation formation, the modification of craze

initiation and propagation in a specific polymer by a given diluent cannot be predicted a priori. The polymer-diluent interactions on a molecular level and the effect of these interactions on plasticization and swelling behavior at the craze tip are not understood. For example, the role of factors, such as the size and shape of the diluent molecule[270,271], the rotational isomeric configurations of the polymer, and the flexibility of the polymer chains in polymer-diluent interactions are not fully understood.

There are a number of additional phenomena that play a significant role in solvent crazing. For an initially undiluted polymer that is stressed in a diluent environment, Williams and coworkers[236,245,253,260,267] have determined that the craze growth rate is controlled by the slower of either the relaxation processes of the polymer or the rate of flow of the diluent through the porous craze structure. Mai and coworkers[265,269] have investigated the effects of diluents on polymer fracture toughness as a function of crack velocity. Hopfenberg and coworkers[214-218] have shown that solvent crazing can be significantly enhanced by any orientation present in the polymer. Crazing has been shown to occur at the boundary between the outer swollen gel and the unpenetrated glassy core of the polymer when the combined orientation and swelling stresses are sufficiently large to cause craze cavitation and propagation. Subtle differences in polymer orientation can result in significant changes in the rate of solvent crazing. These workers also found that crazing can occur upon either sorption or desorption of the diluent from the glassy polymer which depend on variations in the thermal and mechanical histories of the glass.

Distribution of the diluent within the polymer is another significant factor affecting craze initiation and growth characteristics. Andrews and coworkers[231,244,249] assume an initial homogeneous distribution of diluent within the polymer, but in many service environments clustering of the diluent in the polymer may occur. For example, sorption of the diluent into the polymer at elevated temperatures could cause the polymer to be saturated with the diluent. When the polymer is subsequently cooled, the solubility of the diluent in the polymer is lowered, and regions of high diluent concentration or even diluent clusters can form in the polymer.[212,270,271] Dynamic mechanical studies of such polymer-diluent systems suggest that the regions of high diluent concentration are small, $\sim$ 10 nm.[270,271] These regions would preferentially be highly plasticized which would lower the local

shear yield stress and favor cavitation. Within these regions of high diluent concentration, the surface energy associated with void formation would also be lowered if the surface tension of the diluent were lower than that of the polymer.[272,273] It is possible that the regions of high diluent concentration, because of their small size, would favor craze cavitation but not significantly plasticize the craze fibrils. For these conditions, crazes would form more easily, but the fibrils would possess good load-bearing capability. This hypothesis may explain why poor solvents act as good crazing agents because of their tendency to cluster, whereas good solvents act as cracking agents because they are homogeneously distributed throughout the glass thereby plasticizing and softening the craze fibrils.

There have been few studies on the modification of the modes of deformation and failure of thermosets by water.[84,86,88,170,172] Generally, such studies reported changes in fracture toughness induced by water with no attempt to explain such changes in terms of modification of the microscopic modes of deformation and failure.

We have recently studied the effect of sorbed moisture on the tensile mechanical properties and fracture topographies of TGDDM-DDS (27 wt% DDS) epoxy as a function of test temperature. In Figure 28, the tensile strength, ultimate elongation, and Young's modulus of both initially wet and dry epoxies are shown as a function of test temperature. The wet epoxies exhibit lower tensile strengths, ultimate elongations, and moduli than the dry epoxies from room temperature to 150°C. Plasticization of the epoxy including a softening of the craze fibrils by the sorbed moisture would cause such a deterioration in the mechanical properties. Above 150°C, the mechanical properties of both the initially wet and dry epoxies start to merge because significant amounts of moisture are eliminated from the wet glasses during the time of the test.

The microscopic yield stress (that stress at the onset of non-linear behavior in the tensile stress-strain curve) is shown in Figure 29 as a function of test temperature for both initially wet and dry TGDDM-DDS (27 wt% DDS) epoxies. (This yield stress is closely associated with the onset of localized flow and cavitation.) The microscopic yield stress of the wet epoxies is lower than that of the dry glasses from room temperature to 150°C, as shown in Figure 29. Above 150°C, the yield stresses of the wet and dry epoxies merge because water is eliminated from the wet specimens during the test.

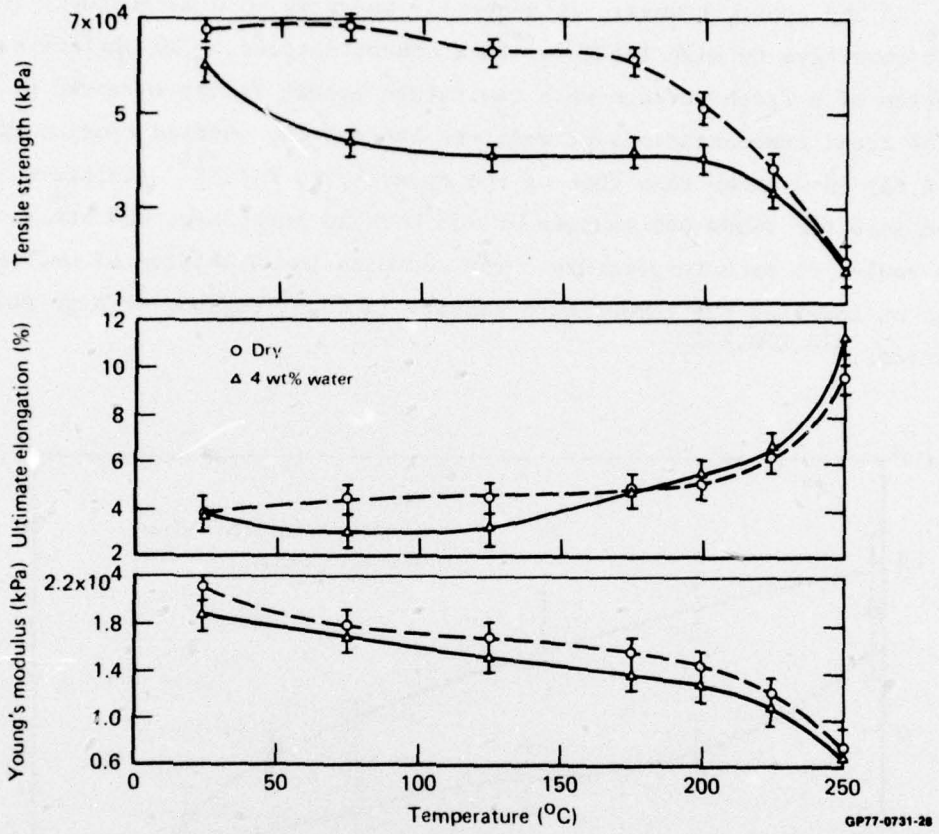

Figure 28 Tensile strength, ultimate elongation, and Young's modulus of initially wet (~4 wt% sorbed moisture) and dry TGDDM-DDS (27 wt% DDS) epoxies as a function of test temperature (strain-rate ~ 10^{-2}/min)

From room temperature to 150°C, the lower yield stresses of the epoxies containing 4 wt% sorbed moisture, relative to those of the dry epoxies, are equivalent to lowering the dry yield stresses 100°-125°C on the temperature scale. However, the T_g of this epoxy is lowered only ∿ 60°C by ∿ 4 wt% sorbed moisture (see Figure 27). These observations imply that craze cavitation stress is more susceptible to sorbed moisture than the main T_g. Hence, the magnitude the T_g is lowered on the temperature scale by sorbed moisture cannot be utilized to predict any modification of the formation of permanent damage regions in these epoxies. The craze cavitational stress is more sensitive to sorbed moisture than the T_g for a heterogeneous distribution of moisture in the epoxy. High moisture concentrations in localized regions enhance cavitation by plasticization which results in a lower local shear yield stress. The

overall T_g of the epoxy, however, is generally measured on a macroscopic level and is not sensitive to high local moisture concentrations. The surface energy for formation of a fresh surface when cavitation occurs is not enhanced by the presence of local concentrations of moisture because the surface tension of water (7.2 Pa) is greater than that of the epoxy($\sim$ 4-5 Pa).[274] (Moisture was introduced into the TGDDM-DDS epoxies at 135°C in an autoclave, and the samples were then cooled to room temperature. The decrease in solubility of moisture in epoxies on lowering the temperature results in local regions of high moisture concentrations.[212,270,271])

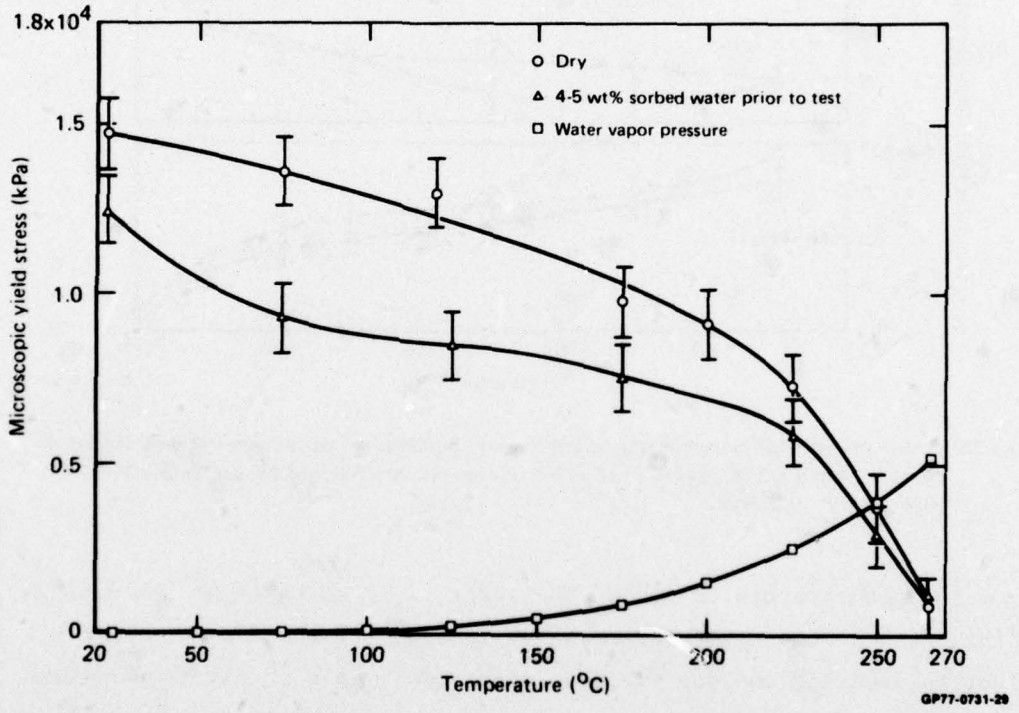

Figure 29 Microscopic yield stress (strain-rate ~ 10^{-2}/min) of initially wet (~4 wt% sorbed moisture) and dry TGDDM-DDS (27 wt% DDS) epoxies and water vapor pressure as a function of temperature

Fracture topography studies also indicate that craze deformation and failure modes in epoxies are modified by sorbed moisture. The optical micrographs in Figure 30 compare the room-temperature fracture topography of a dry TGDDM-DDS (27 wt% DDS) epoxy with one containing $\sim$ 4 wt% sorbed water. The smooth, mirror-like region in the wet sample is considerably larger than in

the dry sample. The extent of the mirror-like region is a measure of the area in which crack propagation occurs through a preformed craze. Hoare and Hull[102] suggested that this area depends on the ease of craze growth, crack nucleation, and crack growth within the craze. The area of the mirror-like region increases with test temperatures as illustrated in Figure 22. The extent of this region in the wet specimen that fractured at room temperature is equivalent to that in a dry specimen fractured at 125°C.

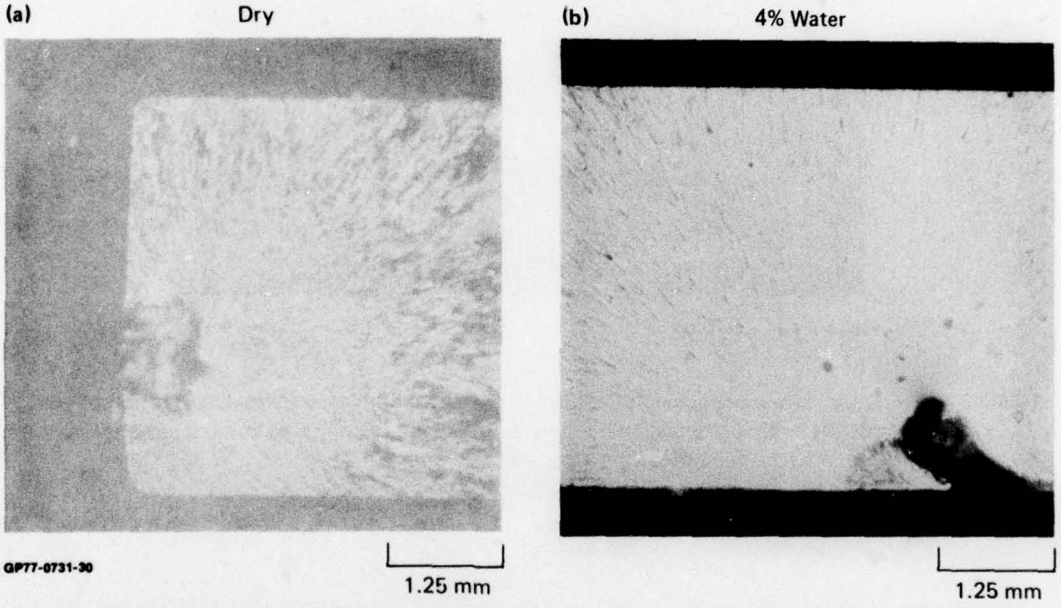

Figure 30 Optical micrographs of room temperature fracture surfaces of (a) dry and (b) (4 wt% sorbed moisture) TGDDM-DDS (27 wt% DDS) epoxy

Scanning electron micrographs of the fracture topography initiation regions in the wet TGDDM-DDS epoxies reveal numerous cavities, as illustrated in Figure 31. The cavities are more numerous than those observed in dry epoxy glasses fractured under similar conditions. This observation suggests that sorbed moisture in these epoxies enhances cavitation.

Hence, the data illustrated in Figures 28-31 suggest that sorbed moisture lowers the craze initiation and propagation stresses in TGDDM-DDS epoxies. The sorbed moisture has a more severe effect on the crazing process than the T_g, probably as a result of the presence of islands of high moisture concentration.

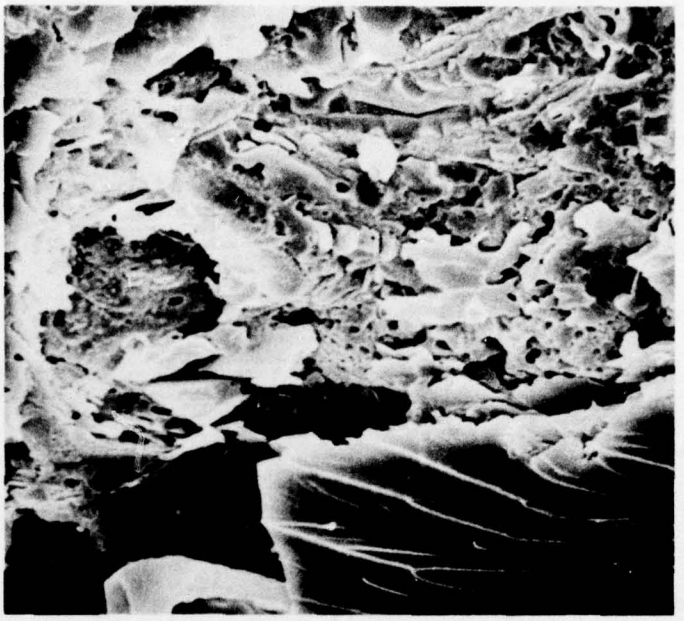

Figure 31 Scanning electron micrograph of cavities in the fracture topography initiation region of wet TGDDM-DDS (27 wt% DDS) epoxy (4 wt% sorbed moisture) which was fractured at room temperature at a strain-rate of $\sim 10^{-2}$/min

The enhancement of craze cavitation and propagation in TGDDM-DDS epoxies by sorbed moisture directly affects the durability of these glasses in humid environments. The plasticizing effect of sorbed moisture on TGDDM-DDS epoxies is already abnormally large (see Section 6.1). However, local concentrations of sorbed moisture lower the local shear yield stress to an even greater extent than that expected from the observed, macroscopic lowering of the T_g. Such high, local moisture concentrations can form in microvoids, in the porous structure of a preformed craze, or from moisture sorption at elevated temperature followed by exposure of the epoxy to lower temperature. The ease of diffusion of moisture through a porous craze structure and its accumulation near the craze tip where it enhances cavitation must be considered a significant mechanism for the growth of permanent damage regions in these glasses in humid environments, particularly in view of the low stress levels at which cavitation generally occurs in polymer glasses (Figure 29).

7. FACTORS THAT CONTROL THE DURABILITY OF EPOXIES

In the service environment, durability of epoxies depends on a complex number of interacting phenomena. The factors that control the critical path to ultimate failure or unacceptable damage depend specifically on the particular environmental conditions. In this section, all possible factors that generally affect the durability of epoxies in service environments are reviewed, and some of the critical environments that affect the durability of epoxies and the difficulties in predicting their long-term durability are discussed.

The durability of an epoxy component depends on the structure and physical state of the epoxy after cure and fabrication. Figure 32 illustrates the primary phenomena that are dependent on cure and fabrication conditions and that also affect the durability of epoxies. These phenomena include the network structure, microvoid characteristics (considered in Section 4), and fabrication stresses. Stresses can arise in the epoxy during fabrication from (1) shrinkage of the epoxy during cure, (2) temperature gradients within the sample during cure, and (3) the mismatch in the coefficients of expansion of the epoxy matrix and fiber in an epoxy composite.[275,276] Temperature gradients, which are worse in thick specimens, can cause one region of the epoxy to form a glass prior to other regions during cure. Once the epoxy has formed a glass at the cure temperature, stresses develop in a composite on cooling to room temperature because of the difference in the coefficients of expansion of matrix and filler. Such stresses are complex and intimately depend on the distribution of the fibers in the epoxy matrix. The theoretical treatment of the stresses and strains that arise from thermal expansion and shrinkage differences in composites has recently been reviewed by Hale.[277] Several environmental factors can cause growth of the flaws produced during cure and fabrication and/or formation of new permanent damage regions. Figure 33 illustrates the environmental factors that contribute to the formation of permanent damage regions and, hence, directly limit the durability of epoxies. The primary environmental factors are service stresses, humidity, temperature, and solar radiation.

Normal service stresses, particularly in combination with environmental and fabrication stresses, can cause formation of permanent damage regions in epoxies. Solar radiation can induce surface crosslinking and/or a lowering of

molecular weight which will cause surface stresses and possible microcracking.[278] (There is no evidence, at present, to suggest that TGDDM-DDS epoxies are particularly susceptible to radiation-induced chemical changes.)

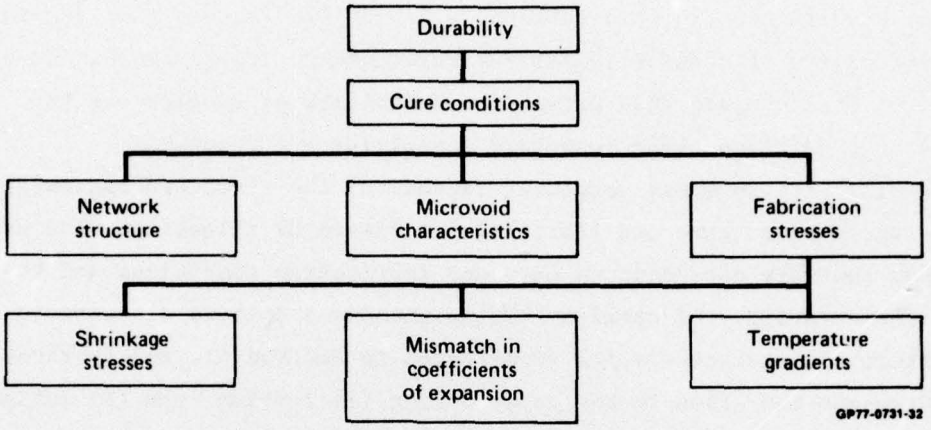

Figure 32 Schematic of cure and fabrication factors that affect the durability of epoxies

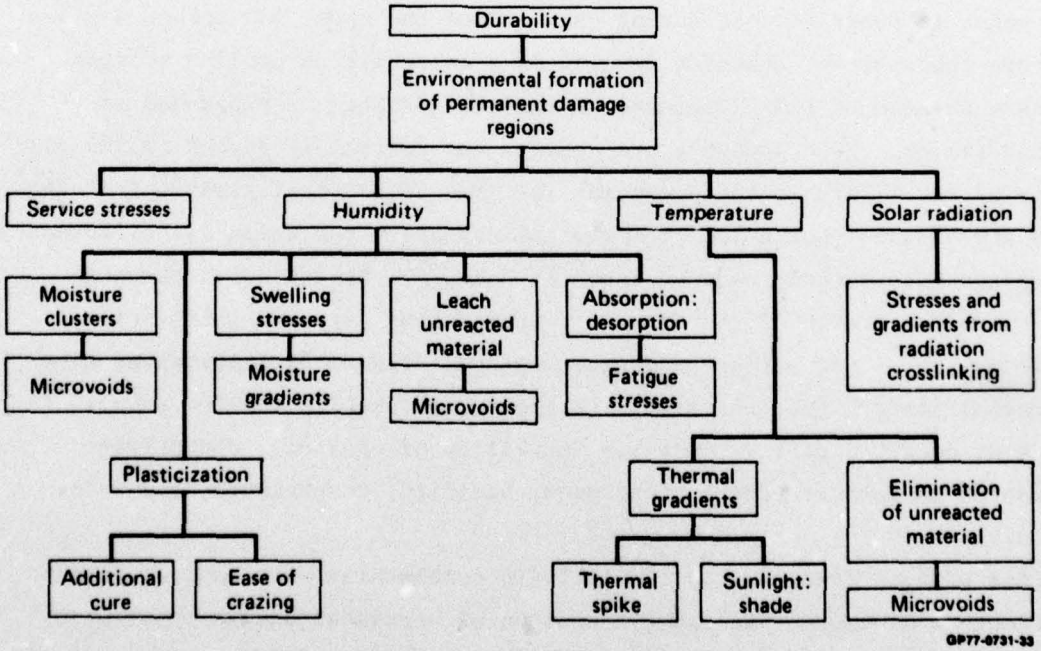

Figure 33 Schematic of environmental factors that affect the durability of epoxies

Temperature effects can also contribute to the formation of permanent damage regions. High temperatures can cause trapped, unreacted, low-molecular-weight material to be evolved from the epoxy, resulting in microvoids (see Section 4.2). Thermal gradients can cause stresses in epoxy components. Such gradients can be caused by sunlight heating only one surface or from a thermal spike caused by aerodynamic heating during high-speed dashes by an aircraft followed by rapid cooling when speed is reduced.

The sorption of moisture by epoxies can cause a number of phenomena which may contribute to the formation of permanent damage regions. Moisture-induced plasticization, in addition to enhancing crazing, increases the mobility within the epoxy which may lead to additional cure. Sorbed moisture causes swelling stresses which are particularly serious at the boundary between the outer swollen region and the inner unswollen core. The sorption and desorption of moisture causes oscillatory swelling stresses which are equivalent to subjecting the epoxy to fatigue. The sorption and desorption of moisture could result in leaching from the epoxy any unreacted, low-molecular-weight material, resulting in microvoids. The formation of water clusters (see Section 6.4) and their subsequent elimination can also result in the formation of microvoids in epoxies. Bair and Johnson[212] have directly shown that cavities are produced in a polyethylene-water system by such a mechanism.

There are many possible critical paths involving the effects of the original network structure, microvoid characteristics, and fabrication stresses together with service stresses, moisture, temperature, and solar radiation exposure of epoxies that will lead to formation and/or growth of permanent damage regions. The critical path that causes damage and that predominates in a given service environment often depends on a complex series of interacting phenomena which were illustrated as separate entities in Figures 32 and 33.

The most extreme environmental conditions experienced by components on a fighter aircraft occur during a supersonic dash. The aircraft dives from high altitudes (outer surface temperature -20° to -55°C) into a supersonic, low-altitude run during which the surface temperature rises in minutes to 100°-150°C as a result of aerodynamic heating. On reduction of speed, the outer surface temperature drops extremely rapidly. In Figure 34, a temperature profile of the outer surface of the aircraft component as a function of time illustrates the thermal spike that the outer surface receives during the

supersonic maneuver. This particular thermal spike has been utilized by McKague[168] and Browning[177] in their studies of the simulation of real-life environmental conditions on the durability of epoxies and epoxy composites. McKague[168] found that epoxy laminates are damaged after thermal-spike exposures as indicated by abnormal increases in moisture sorption. Browning[177] found similar evidence of thermal-spike-induced damage in unfilled TGDDM-DDS epoxies. After exposure to thermal spikes, this epoxy exhibited numerous surface microcracks. Browning[177] suggests that damage occurs during the rapid cool-down portion of the spike at which the rate is $\sim$ 500°C/min. The rapid cool-down rate causes the exterior of the epoxy component to be cooler than the interior, which results in surface tensile stresses. In addition, moisture is driven from the exterior but not from the interior of the component during the temperature-rise portion of the spike, which leads to a moisture gradient. The larger swelling stresses in the interior of the material relative to the less swollen exterior results in surface tensile stresses which, together with those stresses that result from the temperature gradients, are sufficiently large to cause growth of permanent damage regions by a crazing mechanism. During the short duration of the thermal spike, some moisture remains in the epoxy surface region and lowers the craze cavitation stress (see Section 6.4), thereby enhancing the possibility of surface damage.

The less rapid heating rate of the thermal spike could also possibly cause damage as a result of expanding, superheated steam momentarily trapped in a microvoid. At 150°C, a small vapor pressure could cause microvoid expansion because the yield stress of the highly plasticized microvoid walls is negligible at this temperature. (In Figure 29, the water vapor pressure is plotted as a function of temperature; at 150°C the vapor pressure is similar in magnitude to the yield stress of the wet epoxy assuming the dry epoxy yield stress-temperature plot is shifted 100°-125°C on the temperature scale by sorbed moisture.) At MDRL, moisture-saturated epoxies have been rapidly heated by introduction into a preheated oven in the 50-150°C range. Mechanical property and fracture topography observations do not indicate any significant evidence of microvoid growth as a result of water vapor pressure. Therefore, at present, the primary mode of damage during a thermal spike occurs during the rapid cool-down period.

The thermal spike utilized by McKague[168] and Browning[177] is one of the more severe spikes in terms of maximum temperature and rate of cool-down.

Recently, Bohlman and Derby[178] found no evidence of damage in graphite-epoxy laminates for the less-severe thermal spike condition which the Space Shuttle Orbiter will experience (assuming a cool-down rate of only 4°C/min).

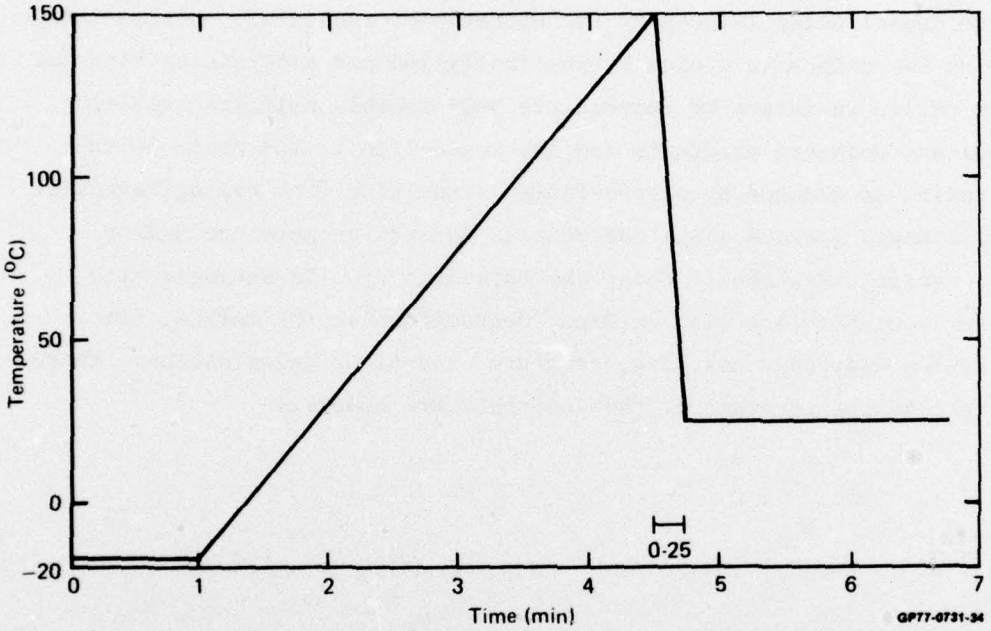

Figure 34 Thermal spike experienced by outer surface of epoxy component as a result of a supersonic maneuver

For less-severe environmental conditions than those that involve supersonic maneuvers, it is, at present, difficult to predict the long-term effects of fabrication and environmental factors on the durability of epoxies in specific environments. Such a priori predictions require knowledge of the structure-property relations of epoxies, the magnitude and/or duration of fabrication, environmental and service stresses placed on the material, and a detailed understanding of other fabrication and environmental factors alluded to in Figures 32 and 33. However, the present state of knowledge of epoxies and composite materials does not yield all such required information.

Furthermore, an understanding of the interactions of the various fabrication and environmental factors that affect the durability of thermosets or their composites has received little attention. Blaga and Yamasaki[159] have

studied and suggested the critical phenomena affecting the weathering of glass-reinforced polyesters. In their studies, they propose that damage occurs in surface regions under the combined action of radiation-induced tensile stresses in the surface region together with physically-induced stress fatigue. Tensile stresses in the surface region are caused by shrinkage of the matrix that results from crosslinking induced by the ultraviolet radiation. Stress fatigue is imposed on the composite system by physically-induced alternating stresses produced by cyclic variation of temperature and probably moisture resulting from thermal and moisture gradients and inhomogeneities. The resin in the interface region is damaged by stress-fatigue resulting from the differential dimensional changes between glass and matrix, induced by moisture and/or temperature cyclic variations. Under the influence of alternating cyclic stresses and in conjunction with chemical degradation of the matrix, the interface region undergoes cracking, fracture, and fiber delamination. These workers note that the stresses at the interface are complex.

ACKNOWLEDGEMENTS

We wish to acknowledge Dr. D. R. Ulrich of the Air Force Office of Scientific Research and Drs. D. P. Ames and C. J. Wolf of McDonnell Douglas Research Laboratories for their support and encouragement of this work.

REFERENCES

1. Air Force Durability Workshop, Battelle Columbus Laboratories, September 1975.
2. Air Force Conference on The Effects of Relative Humidity and Temperature on Composite Structures, University of Delaware, March 1976, AFOSR-TR-77-0030 (1977).
3. J. P. Berry, J. Polymer Sci. 50, 107 (1961).
4. J. P. Berry, J. Polymer Sci. 50, 313 (1961).
5. R. F. Boyer, Rubber Chem. Technol. 36, 1301 (1963).
6. R. P. Kambour, J. Polymer Sci. A3, 1713 (1965).
7. R. P. Kambour, Polymer Eng. Sci. 8, 281 (1968).
8. R. P. Kambour, Appl. Polymer Symposia 7, 215 (1968).
9. J. Heijboer, in Macromolecular Chemistry, O. Wichterle and B. Sedlacek, Eds., (Interscience, New York, 1968), p. 3755.
10. E. H. Andrews, Fracture in Polymers, (Elsevier, New York, 1968).
11. S. M. Aharoni, J. Appl. Polymer Sci. 16, 3275 (1972).
12. S. Rabinowitz and P. Beardmore, in Critical Reviews in Macromolecular Science, (Chem. Rubber Co., Cleveland, 1972), Vol. 1, p. 1.
13. R. J. Morgan, J. Polymer Sci. (Phys. Ed) 11, 1271 (1973).
14. J. R. Kastelic and E. Baer, J. Macromol. Sci. - Phys. B7(4), 679 (1973).
15. R. J. Morgan and L. E. Nielsen, J. Macromol. Sci. - Phys. B9(2), 239 (1974).
16. A. J. Kovacs, Adv. Polymer Sci. 3, 394 (1964).
17. M. H. Litt and A. V. Tobolsky, J. Macromol. Sci. - Phys. B1(3), 433 (1967).
18. R. F. Boyer, Polymer Eng. Sci. 8, 161 (1968).
19. R. J. Morgan and J. E. O'Neal, Polymer and Plast. Tech. and Eng. 5(2), 173 (1975).
20. S. E. B. Petrie, in Polymeric Materials: Relationships Between Structure and Mechanical Behavior, E. Baer and S. V. Radcliffe, Eds., (Am. Soc. for Metals, 1975), p. 55.
21. R. J. Morgan and J. E. O'Neal, J. Polymer Sci. (Polymer Phys. Ed.) 14, 1053 (1976).
22. A. N. Gent, J. Mater. Sci. 5, 925 (1970).
23. E. H. Andrews, in The Physics of Glassy Polymers, R. N. Haward, Ed., (Applied Science Publishers Ltd., 1973) Ch. 7.

24. D. Katz and A. V. Tobolsky, Polymer 4, 417 (1963).
25. T. K. Kwei, J. Polymer Sci. A1, 2977 (1963).
26. A. S. Kenyon and L. E. Nielsen, J. Macromol. Sci.-Chem. A3(2), 275 (1969).
27. R. P. Kreahling and D. E. Kline, J. Appl. Polymer Sci. 13, 2411 (1969).
28. J. P. Bell, J. Polymer Sci. A-2 8, 417 (1970).
29. T. Murayama and J. P. Bell, J. Polymer Sci. A-2 8, 437 (1970).
30. M. A. Acitelli, R. B. Prime, and E. Sacher, Polymer 12, 335 (1970).
31. R. G. C. Arridge and J. H. Speake, Polymer 12, 443 and 450 (1972).
32. P. V. Sidyakin, Vysokomol. soyed. A14, 979 (1972).
33. T. Hirai and D. E. Kline, J. Appl. Polymer Sci. 16, 3145 (1972).
34. R. B. Prime and E. Sacher, Polymer 13, 455 (1972).
35. P. G. Babayevsky and J. K. Gillham, J. Appl. Polymer Sci. 17, 2067 (1973).
36. T. Hirai and D. E. Kline, J. Appl. Polymer Sci. 17, 31 (1973).
37. E. Sacher, Polymer 14, 91 (1973).
38. D. A. Whiting and D. E. Kline, J. Appl. Polymer Sci. 18, 1043 (1974).
39. J. K. Gillham, J. A. Benci, and A. Noshay, J. Appl. Polymer Sci. 18, 951 (1974).
40. L. E. Nielsen, J. Macromol. Sci. Rev. Macromol. Chem. C3(1), 69 (1969).
41. L. E. Nielsen, Crosslinking-Effect on Physical Properties of Polymers, Monsanto/Washington University/ONR/ARPA Association, Report HPC-68-57, May (1968).
42. T. S. Carswell, Phenoplasts, (Interscience, New York, 1947).
43. T. G. Rochow and F. G. Rowe, Anal. Chem. 21, 261 (1949).
44. R. A. Spurr, E. H. Erath, H. Myers, and D. C. Pease, Ind. Eng. Chem. 49, 1839 (1957).
45. E. H. Erath and R. A. Spurr, J. Polymer Sci. 35, 391 (1959).
46. T. G. Rochow, Anal. Chem. 33, 1810 (1961).
47. E. H. Erath and M. Robinson, J. Polymer Sci. C No. 3, 65 (1963).
48. H. P. Wohnsiedler, J. Polymer Sci. C No. 3, 77 (1963).
49. D. H. Solomon, B. C. Loft, and J. D. Swift, J. Appl. Polymer Sci. 11, 1593 (1967).
50. R. E. Cuthrell, J. Appl. Polymer Sci. 11, 949 (1967).
51. A. N. Neverov, N. A. Birkina, Yu. V. Zherdev, and V. A. Kozlov, Vysokomol. soyed. A10, 463 (1968).
52. G. Nenkov and M. Mikhailov, Makromol. Chem. 129, 137 (1969).
53. B. E. Nelson and D. T. Turner, J. Polymer Sci. (Phys. Ed.) 10, 2461 (1972).
54. L. G. Bozveliev and M. G. Mihajlov, J. Appl. Polymer Sci. 17, 1963 and 1973 (1973).

55. R. J. Morgan and J. E. O'Neal, Polymer Preprints 16, No. 2, 610 (1975).
56. K. Selby and L. E. Miller, J. Mater. Sci. 10, 12 (1975).
57. J. L. Racich and J. A. Koutsky, Bull. Am. Phys. Soc. 20, 456 (1975).
58. M. I. Karyakina, M. M. Mogilevich, N. V. Maiorova, and A. V. Udalova, Vysokomol. soyed. A17, 466 (1975).
59. M. V. Maiorova, M. M. Mogilevich, M. I. Karyakina, and A. V. Udalova, Vysokomol. soyed. A17, 471 (1975).
60. V. M. Smartsev, A. Ye. Chalykh, S. A. Nenakhov, and A. T. Sanzharovskii, Vysokomol. soyed. A17, 836 (1975).
61. H. Lee and K. Neville, Handbook of Epoxy Resins, (McGraw-Hill, 1967), Ch.5.
62. J. A. Manson, S. L. Kim, and L. H. Sperling, Influence of Crosslinking on the Mechanical Properties of High T_g Polymers, Technical Report AFML-TR-76-124 (1976).
63. B. Wunderlich and A. Mehta, J. Polymer Sci. - Polymer Phys. Ed. 12, 255 (1974).
64. S. M. Aharoni, J. Appl. Polymer Sci. 19, 1103 (1975).
65. K. Neki and P. H. Geil, J. Macromol. Sci.-Phys. B8(1-2), 295 (1973).
66. A. J. Chompff, Amer. Chem. Soc. Div. Org. Coat. Plast. Preprints 36 (No. 2), 529 (1976).
67. P. J. Flory, Principles of Polymer Chemistry, (Cornell University Press, Ithaca, 1953) Ch. 9.
68. E. G. K. Pritchett, Chem. and Ind. 2, 95 (1949).
69. N. J. L. Megson, Phenolic Resin Chemistry, Academic Press, New York, 1958).
70. D. H. Solomon, J. Macromol. Sci. C1, 179 (1967).
71. R. J. Morgan and J. E. O'Neal, J. Macromol. Sci.-Phys. (in press).
72. J. P. Bell and W. T. McCarvill, J. Appl. Polymer Sci. 18, 2243 (1974).
73. P. L. Jain, J. Polymer Sci. 31, 210 (1958).
74. D. W. Ovenall, J. Polymer Sci. B1, 37 (1963).
75. M. A. Kennan and D. A. Smith, J. Appl. Polymer Sci. 11, 1009 (1967).
76. D. A. Smith, Amer. Chem. Soc. Div. Org. Coat. Plast. Preprints 27, 321 (1967).
77. L. J. Broutman and F. J. McGarry, J. Appl. Polymer Sci. 9, 609 (1965).
78. R. Griffiths and D. G. Holloway, J. Mater. Sci. 5, 302 (1970).
79. R. L. Patrick, W. G. Gehman, L. Dunbar, and J. A. Brown, J. Adhesion 3, 165 (1971).
80. P. B. Bowden and J. A. Dukes, J. Mater. Sci. 7, 52 (1972).

81. R. L. Patrick, in Treatise on Adhesion and Adhesives, R. L. Patrick, Ed., (Dekker, New York, 1973) Vol. 3, p. 163.
82. R. J. Young, P. W. R. Beaumont, J. Mater. Sci. 10, 1343 (1975).
83. R. J. Morgan and J. E. O'Neal, Amer. Chem. Soc. Div. Org. Coat. Plast. Preprints 36 (No. 2), 689 (1976).
84. A. Christiansen and J. B. Shortall, J. Mater. Sci. 11, 1113 (1976).
85. S. Mostovoy and E. J. Ripling, J. Appl. Polymer Sci. 10, 1351 (1966).
86. S. Mostovoy and E. J. Ripling, J. Appl. Polymer Sci. 15, 641 (1971).
87. A. T. DiBennedetto and A. D. Wambach, Int. J. Polymer. Mater. 1, 159 (1972).
88. A. D. S. Diggwa, Polymer 15, 101 (1974).
89. W. D. Bascom, R. L. Cottington, R. L. Jones, and P. Peyser, J. Appl. Polymer Sci. 19, 2545 (1975).
90. P. G. Babayevskii and Ye. B. Trostyanskaya, Vysokomol. soyed. A17, 906 (1975).
91. R. A. Gledhill and A. J. Kinloch, J. Mater. Sci. 10, 1263 (1975).
92. R. J. Morgan and J. E. O'Neal, J. Mater. Sci. (in press).
93. S. S. Sternstein and L. Ongchin, Polymer Preprints 10, 1117 (1969).
94. R. P. Kambour, J. Polymer Sci. Macromol. Rev. 7, 1 (1973).
95. J. Murray and D. Hull, Polymer 10, 451 (1969).
96. S. Rabinowitz, A. R. Krause, and P. Beadmore, J. Mater. Sci. 8, 11 (1973).
97. P. L. Cornes and R. N. Haward, Polymer 15, 149 (1974).
98. J. Murray and D. Hull, J. Polymer Sci. A-2 8, 1521 (1970).
99. P. Beahan, M. Bevis, and D. Hull, J. Mater. Sci. 8, 162 (1972).
100. M. J. Doyle, J. Polymer Sci.-Polymer Phys. Ed. 13, 127 (1975).
101. M. J. Doyle, J. Mater. Sci. 10, 300 (1975).
102. J. Hoare and D. Hull, J. Mater. Sci. 10, 1861 (1975).
103. M. D. Skibo, R. W. Hertzberg, and J. A. Manson, J. Mater. Sci. 11, 479 (1976).
104. J. E. O'Neal, unpublished.
105. G. Pezzin, G. Ajroldi, T. Casiraghi, C. Garbuglio, and G. Vittadini, J. Appl. Polymer Sci. 16, 1839 (1972).
106. R. G. Faulkner, J. Macromol. Sci.-Phys. B11(2), 251 (1975).
107. R. P. Chartoff, Polymer 16, 470 (1975).
108. F. Zandeman, Publs. Scient. Tech. Minist. Air, Paris No. 291 (1954) Ch. IV.
109. S. B. Newman and I. Wolock, J. Appl. Phys. 29, 49 (1958).

110. I. Wolock and S. B. Newman, in Fracture Processes in Polymeric Solids, B. Rosen, Ed., (Interscience, 1964) Ch. II c.
111. R. J. Bird, J. Mann, G. Pogany, and G. Rooney, Polymer 7, 307 (1966).
112. M. J. Owen and R. G. Rose, J. Mater. Sci. 10, 1711 (1975).
113. M. J. Doyle, J. Mater. Sci. 10, 159 (1975).
114. H. El-Hakeem, G. P. Marshall, E. I. Zichy, and L. E. Culver, J. Appl. Polymer Sci. 19, 3093 (1975).
115. R. J. Morgan and J. E. O'Neal, Amer. Chem. Soc. Div. Org. Coat. Plast. Preprints 37 (No. 2) (1977) (in press).
116. R. N. Haward, B. M. Murphy, and E. F. T. White, J. Polymer Sci. A-2 9, 801 (1971).
117. D. Hull, Acta Met. 8, 11 (1960).
118. N. J. Mills, J. Mater. Sci. 11, 363 (1976).
119. H. W. Eickner, Environmental Exposure of Adhesive-Bonded Metal Lap Joints, Technical Report WADC-TR-59-564 (1960).
120. K. E. Kimball, Forest Products Laboratory, Technical Report No. WADC-TR-55-319 (1962).
121. G. Epstein and W. Banderuk, The Crazing Phenomena and Its Effects in Filament-Wound Vessels, 19th Annual Technical Conference, Society of Plastics Industries, Reinforced Plastics Division (1964).
122. J. A. Kies, The Strength of Glass Fibers and the Failure of Filament Wound Pressure Vessels, Naval Research Laboratory Report 6034 (1964).
123. G. R. Irwin, Moisture Assisted Slow Crack Extension in Glass Plates, Naval Research Laboratory Memorandum Report 1678 (1966).
124. L. H. Sharpe, Appl. Polymer Symp. 3, 353 (1966).
125. I. G. Romanenkov and Z. P. Machavariari, Soviet Plast. 5, 49 (1966).
126. K. H. G. Ashbee, F. C. Frank, and R. C. Wyatt, Proc. Roy. Soc. A300, 415 (1967).
127. D. J. Steel, Trans. Plast. Inst. 35, 116 and 429 (1967).
128. I. G. Romanenkov, Soviet Plast. 6, 74 (1967).
129. J. L. Parham and E. A. Verchot, U. S. Army Missile Command Report No. RS-TR-67-6 (1967).
130. N. C. W. Judd, Royal Aircraft Establishment, Farnborough, Final Report RAE-TR-67042 (1967).
131. I. Wolcock and H. P. Ewing, Proceedings of 12th National SAMPE Meeting (1967).

132. R. Slysh, Org. Coatings Plast. Chem. Preprints 28 (1), 456 (1968).
133. J. R. Griffith and J. E. Quick, Ibid, 28 (1), 476 (1968).
134. L. A. Liebowitz, Ibid, 28 (1) 479 (1968).
135. D. I. James, R. H. Norman, and M. H. Stone, Plastics and Polymers 36, 21 and 121 (1968).
136. V. R. Dietz, Interaction of Water Vapor with Pristine E-Glass Fiber, Naval Research Laboratory Report 6812 (1968).
137. J. C. Halpin and N. J. Pagano, Proceedings 6th Annual Meeting Society Engineering Science, (Springer-Verlag, New York, 1969).
138. J. L. Parham, U. S. Army Missile Command Report No. RS-TR-70-8 (1970).
139. T. R. Walton and J. E. Cowling, Naval Research Laboratory Report 7077 (1970).
140. N. Fried, in Mechanics of Composite Materials, F. W. Wendt, H. Leibowitz, and N. Perrone, Eds., (Pergamon, New York, 1970), p. 813.
141. J. L. Parham, U. S. Army Missile Command Report No. RL-TR-71-S (1971).
142. R. B. Bonk and D. A. Teetsel, Picatinny Arsenal Technical Report 2102 (Addendum No. 9) (1971).
143. P. W. R. Beaumont and B. Harris, The Effects of Environment or Fatigue and Crack Propagation in Carbon-Fibre-Reinforced Epoxy Resin, Plastics Institute, International Conference on Carbon Fibres, Their Composites and Applications, London, Paper 49, A71-20892 (1971).
144. M. L. Sartelli and R. A. Simon, Proceedings of the 26th SPI Annual Conference (1971).
145. Convair Aerospace Final Report, Development of Design Data for Graphite Reinforced Epoxy and Polyimide Composites, Contract NASA-26198, NASA-MSFC (1970-71).
146. Convair Aerospace Final Report, Advanced Composite Applications for Spacecraft and Missiles, Contract F33615-70-C-1442 AFML (1970-71).
147. J. C. Leslie, Hercules Analysis of the Composite Aging Problem, Report No. H400-12-1-6 (1971).
148. C. E. Browning, The Effects of Moisture on the Properties of High Performance Structural Resins and Composites, Project No. 7340 AFML (1971).
149. A. P. Penton and J. L. Perry, Investigation on Graphite Filament Reinforced Plastic Composites, Philco-Ford, Aero. Div. Final Report, Contract No. N00019-70-C-0439 (1971).
150. R. D. Edzell, The Effects of Moisture Sorption on Epoxies, Naval Ordnance Laboratory Report NOLTR72-108 (1972).

151. H. L. Young and W. L. Greever, 6th St. Louis Symposium, Composite Materials in Engineering (1972).

152. W. L. Greever, High-Temperature Strength Degradation of Composites During Ambient Aging, Hercules, Inc., Final Report, Contract No. 70-000-22 to General Dynamics, Convair Contract NAS 8-27435 (1972).

153. L. M. Lackman, D. O. Losee, J. A. Rohlen, and T. T. Matoi, Advanced Composites Data for Aircraft Structural Design, AFML-TR-70-58 (1972).

154. C. E. Browning, The Effects of Moisture on the Properties of High Performance Epoxy Resins and Composites, Technical Report AFML-TR-72-94 (1972).

155. J. R. Romans, A. G. Sands, and J. E. Cowling, Ind. Eng. Chem. Prod. Res. Develop. 11, No. 3, 261 (1972).

156. J. Hertz, Investigation into the High-Temperature Strength Degradation of Fiber-Reinforced Resin Composites During Ambient Aging, General Dynamics, Convair, Final Report GDCA-DBG73-005, Contract NAS 8-27435 (1973).

157. C. E. Browning and J. M. Whitney, The Effects of Moisture on the Properties of High Performance Structural Resins and Composites, Society of the Plastics Industry, Reinforced Plastics Division, Proceedings of the 28th Annual Technical Conference, Washington, D.C. (1973).

158. J. F. Carpenter, Moisture Sensitivity of Epoxy Composites and Structural Adhesives, McDonnell Aircraft Report MDC A2640 (1973).

159. A. Blaga and R. S. Yamasaki, J. Mater. Sci. 8, 654 and 1331 (1973).

160. K. E. Hofer, Jr., N. Rao, and D. Larsen, Development of Engineering Data on the Mechanical and Physical Properties of Advanced Composite Materials, Technical Report AFML-TR-72-205 (1974).

161. J. L. Kardos, M. J. Michno, Jr., and T. A. Duffy, Investigation of High Performance Short Fiber Reinforced Plastics, Washington Univ., Naval Air Systems Command Final Technical Report, Contract No. N00019-73-0358 (1974).

162. C. E. Browning, Effects of Moisture on the Properties of High Performance Structural Resins and Composites, Composite Materials-Testing and Design, 3rd Conference, ASTM, ASTM STP546, p. 284 (1974).

163. D. H. Kaeble, P. J. Dynes, L. W. Crane, and L. Maus, J. Adhesion 7, 25 (1975).

164. O. Ishai, Polymer Eng. Sci. 15, 486 and 491 (1975).

165. R. M. Verette, Temperature/Humidity Effects on the Strength of Graphite/Epoxy Laminates, AIAA Paper No. 75-1011 (1975).

166. E. L. McKague, Jr., J. E. Halkias, and J. D. Reynolds, J. Composite Materials 9, 2 (1975).

167. D. A. Scola, A Study to Determine the Mechanisms of S-Glass/Epoxy Resin Composite Degradation Due to Moisture and Solvent Environments, The Society of Plastics Industry, 30th Annual Technical Conference, Reinforced Plastics/Composites Institute (1975).

168. E. L. McKague, Life Assurance of Composite Structures, Technical Report AFML-TR-75-51 (1975).

169. C. H. Shen and G. S. Springer, J. Composite Materials 10, 2 (1976).

170. G. Pritchard, R. G. Rose, and N. Taneja, J. Mater. Sci. 11, 718 (1976).

171. G. A. Pogany, Polymer 17, 690 (1976).

172. R. J. Young and P. W. R. Beaumont, J. Mater Sci. 11, 776 (1976).

173. Y. Weitsman, J. Composite Materials 10, 193 (1976).

174. C. E. Browning, G. E. Husman, and J. M. Whitney, Moisture Effect in Epoxy Matrix Composites, Composite Materials - Testing and Design, 4th Conference, ASTM STP (1976).

175. AFML/AFOSR, Mechanics of Composites Review, Dayton (1976).

176. R. L. Levy, Mechanism by which Moisture Influences the Elevated Temperature Properties of Epoxy Resins, Technical Report AFML-TR-76-190 (1976).

177. C. E. Browning, The Mechanism of Elevated Temperature Property Losses in High Performance Structural Epoxy Resin Matrix Materials after Exposures to High Humidity Environments, Ph.D. Thesis, University of Dayton (1976).

178. R. E. Bohlmann and E. A. Derby, Moisture Diffusion in Graphite/Epoxy Laminates: Experimental and Predicted, AIAA Paper No. 77-399 (1977).

179. R. L. Levy, Mechanism of Epoxy Moisture Effects, Technical Report AFML-TR-77-41 (1977).

180. M. L. Williams, R. F. Landel, and J. D. Ferry, J. Am. Chem. Soc. 77, 3701 (1955).

181. F. Bueche, J. Chem. Phys. 24, 418 (1956).

182. M. H. Cohen and D. Turnbull, J. Chem. Phys . 31, 1164 (1959).

183. F. N. Kelley and F. Bueche, J. Polymer Sci. 50, 549 (1961).

184. L. G. Dowell and A. P. Rinfret, Nature, London, 188, 1144 (1960).

185. M. Sugisaki, H. Suga, and S. Seki, Bull. Chem. Soc. Japan 41, 2591 (1968).

186. A. Korosi and B. M. Fabus, Anal. Chem. 40, 157 (1968).
187. N. H. Fletcher, The Chemical Physics of Ice, (Cambridge Univ. Press, 1970), Ch. 3.
188. R. Frank, Water, (Plenum Press, New York, 1972), Vol. 1.
189. Y. Y. Tan and G. Challa, Polymer 17, 739 (1976).
190. L. E. Nielsen, Mechanical Properties of Polymers, (Reinhold, New York, 1962), p. 27.
191. J. Crank, The Mathematics of Diffusion, (Clarendon Press, Oxford, 1957).
192. C. J. Van Amerongen, Rubber and Chem. Tech. 37, 871 (1964).
193. A. J. King, Multicomponent Diffusion (1-D), Hercules Corporation, Computer Program User's Manual No. 61014 (1976).
194. J. Crank and G. S. Park, Diffusion in Polymers, (Academic Press, London, 1958), Ch. 5.
195. E. W. Russel, Nature 165, 91 (1950).
196. I. Narisawa, J. Polymer Sci. A-2 10, 1789 (1972).
197. D. A. Blackadder and J. S. Keniry, J. Appl. Polymer Sci. 17, 351 (1973).
198. C. H. M. Jacques, H. B. Hopfenberg, and V. Stannett, Polymer Eng. Sci. 13, 81 (1973).
199. C. Clark-Monks and B. Ellis, J. Colloid Interface Sci. 44, 37 (1973).
200. H. Yasuda and A. Peterlin, J. Appl. Polymer Sci. 17, 433 (1973).
201. Y. J. Chang, C. T. Chen, and A. V. Tobolsky, J. Polymer Sci. (Polymer Phys. Ed.) 12, 1 (1974).
202. G. Skirrow and K. R. Young, Polymer 15, 771 (1974).
203. D. R. Paul, J. Polymer Sci. A-2 7, 1811 (1969).
204. E. Drioli, L. Nicolais, and A. Ciferri, J. Polymer Sci. (Polymer Chem. Ed.) 11, 3327 (1973).
205. H. Hoso and W. N. Findley, Polymer Eng. Sci. 13, 225 (1973).
206. S. A. Steen, S. K. Sen, and A. K. Rao, J. Macromol. Sci. B 10, 507 (1974).
207. Z. Miyagi and H. Tanaka, Polymer 16, 441 (1975).
208. P. E. Rouse, Jr., J. Am. Chem. Soc. 69, 1068 (1947).
209. R. M. Barrer and J. A. Barrie, J. Polymer Sci. 28, 377 (1958).
210. J. A. Barrie and D. Machin, Trans. Faraday Soc. 67, 244 (1971).
211. K. Matsushige, E. Baer, and S. V. Radcliffe, J. Macromol. Sci.-Phys. B11(4), 565 (1975).
212. H. E. Bair and G. E. Johnson, Analytical Calorimetry, R. S. Porter and J. F. Johnson, Eds., (Plenum Press, 1976), Vol. 4.

213. D. C. Ruhmann and E. M. Wu, Amer. Chem. Soc. Div. Org. Coat. Plast. Preprints 31 (No. 1), 501 (1971).

214. A. S. Michaels, H. J. Bixler, and H. B. Hopfenberg, J. Appl. Polymer Sci. 12, 991 (1968).

215. H. B. Hopfenberg, R. H. Holley, and V. T. Stannett, Polymer Eng. Sci. 9, 242 (1969).

216. R. H. Holley, H. B. Hopfenberg, and V. T. Stannett, Polymer Eng. Sci. 10, 376 (1970).

217. B. R. Baird, H. B. Hopfenberg, and V. T. Stannett, Polymer Eng. Sci. 11, 4 and 274 (1971).

218. C. H. M. Jacques, H. B. Hopfenberg, and V. Stannett, J. Appl. Polymer Sci. 18, 223 (1974).

219. R. S. Stein and A. V. Tobolsky, Text. Res. J. 18, 302 (1948).

220. L. R. G. Treloar, The Physics of Rubber Elasticity, (Clarendon Press, Oxford, 1958), 2nd. Ed.

221. B. H. Zimm and J. L. Lundberg, J. Phys. Chem. 13, 276 (1956).

222. A. H. Gent and T. H. Kuon, Macromolecules 2, 262 (1969).

223. A. H. Gent and T. H. Kuon, J. Polymer Sci. A2 9, 927 (1971).

224. S. S. Sternstein, J. Macromol. Sci. B6(1), 243 (1972).

225. D. G. LeGrand, J. Appl. Polymer Sci. 20, 1573 (1976).

226. C. Gurney and Z. Borysowsky, Proc. Phys. Soc. A61, 446 (1948).

227. B. Maxwell and L. F. Rahm, Ind. Eng. Chem. 41, 1988 (1949).

228. J. J. Benbow, Proc. Phys. Soc. B78, 970 (1961).

229. H. A. Stuart, G. Markowski, and D. Jeschke, Kunststoffe 54, 618 (1964).

230. J. B. Howard, in Engineering Design for Plastics, E. Baer, Ed., (Reinhold, New York, 1964), p. 742.

231. E. H. Andrews and L. Bevan, Physical Basis of Yield and Fracture, (Institute of Physics, London, 1966), p. 209.

232. C. Gurney and J. Hunt, Proc. Roy. Soc. London A299, 509 (1967).

233. G. A. Bernier and R. P. Kambour, Macromolecules 1, 393 (1968).

234. R. J. Bergen, Jr., SPE J. 24, 77 (1968).

235. I. S. Lyakhovich, I. N. Musayelyan, and N. M. Chirkov, Vysokomol. Soedin. A10, 715 (1968).

236. G. P. Marshall, L. E. Culver, and J. G. Williams, Proc. Roy. Soc. A 319, 165 (1970).

237. G. Menges and H. Schmidt, Plastics and Polymers 38, 13 (1970).

238. G. P. Marshall, L. E. Culver, and J. G. Williams, Plastics and Polymers 38, 95 (1970).

239. R. P. Kambour, E. E. Romagosa, and C. L. Gruner, Macromolecules 5, 335 (1972).

240. P. I. Vincent and S. Raha, Polymer 13, 283 (1972).

241. M. F. Parrish and N. Brown, Nature (Physical Sci.) 237 (77), 122 (1972).

242. N. Brown and M. F. Parrish, J. Polymer Sic. B 10, 777 (1972).

243. A. Hiltner, J. A. Kastelic, and E. Baer, in Advances in Polymer Science and Engineering, K. D. Pae, D. R. Morrow, and Yu Chen, Eds., (Plenum Press, New York, 1972), p. 335.

244. E. H. Andrews and L. Bevan, Polymer 13, 337 (1972).

245. I. D. Graham, G. P. Marshall, and J. G. Williams, Proc. Int. Conf. Dynamic Crack Propagation, (Noordhoff, Leyden, 1972), p. 261.

246. H. G. Olf and A. Peterlin, Polymer 14, 78 (1973).

247. N. Brown, J. Polymer Sci. (Polymer Phys. Ed.) 11, 2099 (1973).

248. S. Fischer and N. Brown, J. Appl. Phys. 44, 4322 (1973).

249. E. H. Andrews, G. M. Levy, and J. Willis, J. Mater. Sci. 8, 1000 (1973).

250. R. P. Kambour, C. L. Gruner, and E. E. Romagosa, J. Polymer Sci. (Polymer Phys. Ed.) 11, 1879 (1973).

251. H. G. Olf and A. Peterlin, J. Polymer Sci. (Polymer Phys. Ed.) 12, 2209 (1974).

252. E. H. Andrews and G. M. Levy, Polymer 15, 599 (1974).

253. J. G. Williams, G. P. Marshall, I. Graham, and E. L. Zichy, Pure Appl. Chem. 39, 275 (1974).

254. G. P. Marshall and J. G. Williams, in Deformation and Fracture of High Polymers, H. H. Kausch, J. A. Hassell, and R. I, Jaffee, Eds., (Plenum Press, New York, 1974), p. 557.

255. D. McCammond and C. A. Ward, Polymer Eng. Sci. 14, 831 (1974).

256. B. L. Earl, R. J. Loneragan, J. Markham, and M. Crook, J. Appl. Polymer Sci. 18, 245 (1974).

257. B. L. Earl, M. Crook. R. J. Loneragan, J. H. T. Johns, and J. Markham, J. Appl. Polymer Sci. 18, 857 (1974).

258. Y. W. Mai, J. Mater. Sci. 9, 1896 (1974).

259. J. R. Martin and J. F. Johnson, J. Appl. Polymer Sci. 18, 3227 (1974).

260. J. G. Williams and G. P. Marshall, Proc. Roy. Soc. London A 342, 55 (1975).

261. N. Brown and Y. Imai, J. Appl. Phys. 46, 4130 (1975).
262. N. Brown and Y. Imai, J. Polymer Sci. B 13, 511 (1975).
263. A. Peterlin and H. G. Olf, J. Polymer Sci. C, No. 50, 243 (1975).
264. G. W. Weidmann and J. G. Williams, Polymer 16, 921 (1975).
265. Y. W. Mai, J. Mater. Sci. 10, 943 (1975).
266. Y. Imai and N. Brown 11, 417 and 425 (1976).
267. I. D. Graham, J. G. Williams, and E. L. Zichy, Polymer 17, 439 (1976).
268. Y. W. Mai, J. Mater. Sci. 11, 303 (1976).
269. Y. W. Mai and A. G. Atkins, J. Mater. Sci. 11, 677 (1976).
270. R. J. Morgan, L. E. Nielsen, and R. Buchdahl, Polymer Preprints 12, 687 (1971).
271. R. J. Morgan and L. E. Nielsen, J. Polymer Sci. A-2 10, 1575 (1972).
272. G. R. Irwin, Handbuch der Physik, (Springer, Berlin, 1958), p. 551.
273. J. C. Fisher, J. Appl. Phys. 19, 1062 (1948).
274. E. G. Shafrin, in Polymer Handbook, J. Brandrup and E. H. Immergut, Eds., (J. Wiley, New York, 1975), Ch. III-221.
275. L. E. Nielsen and T. B. Lewis, J. Polymer Sci. A-2 7, 1705 (1969).
276. R. J. Morgan, J. Mater. Sci. 9, 1219 (1974).
277. D. K. Hale, J. Mater. Sci. 11, 2105 (1976).
278. A. Blaga and R. S. Yamasaki, J. Mater. Sci. 11, 1513 (1976).

DISTRIBUTION LIST

Donald L. Ball
Directorate of Chemical Sciences
Air Force Office of Scientific
Research (AFSC)
Bolling Air Force Base
Building 410
Washington, DC 20332

Charles F. Bersch
Non-Metals Section (Air-52032)
Naval Air Systems Command
Washington, DC 20361

John O. Brittain
Materials Research Center
Northwestern University
Evanston, IL 60201

Ralph A. Britton
McDonnell Aircraft Company
Dept 247, Building 32, Level 2
St. Louis, MO 63166

Charles E. Browning
Structural Composites (MBC)
Air Force Materials Laboratory
Wright-Patterson Air Force Base,
Ohio 45433

T. T. Chiao
University of California
Lawrence Livermore Laboratory
P.O. Box 808
Livermore, CA 94550

Oliver F. Danielson
Manager, Technical Integration
McDonnell Douglas Corporation
Dept H200, Headquarters
St. Louis, MO 63166

Hari Dharan
Ford Aerospace and Communications Corp.
3939 Fabian Way
Mail Stop G-97
Palo Alto, CA 94303

Ramon A. Garrett
McDonnell Douglas Astronautics Co.-East
Dept E452, Building 106, Level 2
St. Louis, MO 63166

Ivan J. Goldfarb
Air Force Materials Laboratory
Nonmetallic Materials Division
Polymer Branch
Wright-Patterson Air Force Base, OH 45433

John C. Halpin
Advanced Composite Technologh (FB)
Air Force Flight Dynamics Laboratory
Wright-Patterson Air Force Base, OH 45433

Thomas V. Hinkle
McDonnell Aircraft Co.
Dept 234, Building 32, Level 2
St. Louis, MO 63166

John Hurt
U.S. Army Research Office
P. O. Box 12211
Research Triangle Park, NC 27709

Raymond J. Juergens
McDonnell Aircraft Co.
Dept. 247, Building 32, Level 2
St. Louis, MO 63166

David H. Kaeble
Rockwell International Science Center
1049 Camino Dos Rios
Thousand Oaks, CA 91360

Frank E. Karasz
Polymer Science and Engineering
Materials Research Laboratory
Office of the Director
University of Massachusetts
Amherst, MA 01003

John L. Kardos
Materials Research Laboratories
Chemical Engineering Dept.
Washington University
Box 1087
St. Louis, MO 63130

John A. Manson
Materials Research Center
Lehigh University
Bethlehem, PA 18015

Clayton May
Lockheed Missiles and Space Co,
P.O. Box 504
Sunnyvale, CA 94088

George Mayer
Metallurgy and Materials Sciences
U.S. Army Research Office
P. O. Box 12211
Research Triangle Park, NC 27709

A. Keith Miller
Dept. of Mechanical Engineering
University of Wyoming
Laramie, WY 82071

Larry Peebles
Office of Naval Research
495 Summer Street
Boston, MA 02210

Jerry Peck
McDonnell Douglas Astronautics CO.-W
Dept. 220, Section ABCO
Mail Stop 13-3
5301 Bolsa Ave.
Huntington Beach, CA 92647

Richard A. Pride
Composites Section
NASA-Langley Research Center
Hampton, VA 23665

Brian Quinn
Director-Aerospace Sciences (NA)
Air Force Office of Scientific Research
Bolling Air Force Base
Washington, DC 20332

Theodore J. Reinhart
Plastics Branch
Air Force Materials Laboratory
Wright-Patterson Air Force Base, OH 45433

N. S. Schneider
Polymer and Chemistry Division
Army Materials and Mechanics Research Ctr.
Watertown, MA 02172

Simon Strauss
Headquarters, AFSC/DL
Andrews AFB, DC 20334

George R. Thomas
DRXMR-R, Organic Materials Laboratory
Army Materials/Mechanics Research Center
Watertown, MA 02172

Charles Tiffany
Aeronautical Systems Division
(ASD-EN)
Wright-Patterson Air Force Base, OH 45433

Hank M. Toellner
Dept. 253, Location C1
Mail-Code 1-18
Douglas Aircraft Co.
3855 Lakewood Blvd.
Long Beach, CA 90846

Stephen Tsai
Mechanics and Surface Interaction
Branch (MBM)
Air Force Materials Laboratory
Wright-Patterson Air Force Base, OH 45433

R. L. Van Deusen
Polymer Branch
Nonmetallic Materials Division
Air Force Materials Laboratory
Wright-Patterson Air Force Base, OH 45433

William J. Walker
Air Force Office of Scientific Research
Bldg. 410
Bolling Air Force Base
Washington, DC 20332

Richard J. Wilkins
General Dynamics
P.O. Box 748
Fort Worth, Texas 76101

Kenneth Wynne
Office of Naval Research
800 N. Quincy Street
Arlington, VA 22217

Defense Documentation Center 2 Cys
Cameron Station
Alexandria, VA 22314